IEEE Access
Multidisciplinary | Rapid Review | Open Access Journal

Received February 4, 2021, accepted February 12, 2021, date of publication February 16, 2021, date of current version February 24, 2021.

Digital Object Identifier 10.1109/ACCESS.2021.3059766

Stability-Based Controller Design of Cloud Control System With Uncertainties

SHOUPING GUAN AND SENLIN NIU
College of Information Science and Engineering, Northeastern University, Shenyang 110819, China
Corresponding author: Senlin Niu (niusenlin_neu@163.com)

This work was supported by the National Natural Science Foundation of China under Grant 61573087.

ABSTRACT A cloud control system (CCS) is inherently uncertain due to the dynamic services and resources in cloud computing. In this paper, an approach of modeling and controller design for CCS is proposed that considers the uncertainties existing in the controlled plant, network, and controller simultaneously; then, a general framework for modeling and controlling uncertain control systems is constructed. First, a typical CCS structure is presented, and the uncertainties in the CCS are analyzed and decomposed. On this basis, a generalized uncertain state-space model is established, which includes the interval controlled plant and the stochastic network, considering the time-delay and packet loss. Meanwhile, the cloud controller model with interval parameters and stochastic time-delay is designed, which includes the state observer and control law. Then, based on the Lyapunov stability theorem and the linear matrix inequality (LMI) method, a stability criterion for obtaining the parameters of the cloud controller is proposed, in which all the results are expressed in the form of the LMI. Finally, simulation results show the effectiveness and generalization performance of the designed cloud controller.

INDEX TERMS Cloud control system (CCS), cloud computing, cloud controller, uncertainty analysis, linear matrix inequality (LMI).

I. INTRODUCTION

The rapid development of information and communication technology and its deep integration with the manufacturing industry have led to major changes in the manufacturing mode, manufacturing process, manufacturing means, ecosystem, etc., and traditional industrial control technologies are facing a new challenge. At present, the conventional control systems, including the integrated control system (ICS), distributed control system (DCS), fieldbus control system (FCS), and networked control system (NCS), have their own advantages and scope of application, but the common problems are shown in their high cost of construction, operation, and maintenance, and the inflexible replacement of the control algorithm [1]–[3]. In recent years, the emergence of cloud computing [4] has brought new ideas to industrial control.

Cloud computing provides dynamically scalable and inexpensive distributed computing capabilities through the network and includes parallel computing, distributed computing, and grid computing [5]. Cloud computing is the result of the hybrid evolution of the concepts of virtualization, utility computing, infrastructure as a service (IaaS), platform as a service (PaaS), and software as a service (SaaS) [6], [7], which can reach 10 trillion operations per second. In an actual cloud computing system, many computers are connected through the network and virtualized into a configurable shared resource pool including computing, software, data access, and storage services. Then, the computing tasks are loaded into the resource pool to complete the calculation [8]. End-users can use it without knowing the details of actual cloud infrastructures, having the corresponding expertise, or knowing the physical location and specific configuration of the service provider. In this system, computers and other devices provide a service through the network, which enables users to access and use them for resource sharing, software use, and information reading, as if the devices were installed locally. With the continuous improvement of the processing capacity of cloud computing systems, the processing burden of the user terminal can be reduced. Finally, the user terminal can be simplified as a pure input and output device, and the user can purchase services on demand.

In the industrial control scheme, cloud computing is introduced to form the cloud control system (CCS) to realize the interaction between computing and control theory [9]. In the

The associate editor coordinating the review of this manuscript and approving it for publication was Guangdeng Zong.

cloud, various intelligent learning algorithms, advanced control algorithms, and data-driven modeling methods can be used to realize the autonomous intelligent control of the system while using high-speed communication channels to ensure the real-time control of the system [10]. The control strategy can be provided as the cloud computing service, that is, the idea of ''control as a service (CaaS)'' [11], [12], which allows the execution of intensive algorithms in the cloud [13]. The most typical feature of CCS is that the controller algorithm is placed in the cloud to form the cloud-based remote control. If the cloud is replaced by a computer, it has a typical NCS structure. Therefore, the CCS will be the next generation of remote control systems after NCS. Due to the virtualization of the controller and the reduction of the hardware and related labor costs, the CCS can significantly reduce the cost and time of the building control system [14] and can flexibly select the control algorithm in the cloud controller according to the different states of different controlled plants to realize ''customized'' control.

The characteristics of cloud computing, such as virtualization, multi-granularity (node), dynamic scheduling, and soft computing, make it more efficient, open, and scalable. However, there are deficiencies in security, reliability, computing, and communication performance. These issues make cloud computing uncertain [15], adding a new challenge to the design of CCS. Reducing the impact of uncertainty on the performance, reliability, security, and robustness of CCS has become a new research topic. This can be studied from two aspects. First, we can put forward novel dynamic resource management strategies, security protection strategies, cloud infrastructure improvement strategies, and service software optimization from the perspective of cloud computing, and improve the performance of CCS by continuously improving the quality of cloud computing, that is, control of the cloud, which is the main research direction at present [16]. Second, from the control point of view, we can design the control algorithm with enough robustness to compensate for the impact of uncertainty, fully considering various uncertainties (cloud computing, network transmission, etc.), so as to improve the performance of the CCS, that is, control through the cloud. However, there is currently less research in this area.

As an extension of NCS, the concept of cloud control system was discussed in [2], [17], and a rudiment of cloud control system was proposed. Furthermore, the advantages and challenges of cloud control system were introduced in [10], [18]. Mahmoud MS *et al.* proposed the architecture of the industrial automation system based on the cloud [19], as well as the possible problems of network time-delay, data loss, and vulnerability to attack [20]. Some scholars have studied the security problem of the CCS where the physical network between cloud and control system is attacked, and put forward defense strategies to resist these attacks [21]–[23]. In [24], an interactive real-time SCADA platform for the CCS was proposed to receive and monitor scalar and matrix data from different cloud nodes in real time and adjust the parameters of the CCS online. In [25], the parallel processing performance of the CCS was analyzed and optimized by using the maximum plus algebra method, according to performance indices of the parallel processing system, such as the clock period, throughput, and task completion time. Reference [26] analyzed the network communication requirements of the CCS under different usage backgrounds, and proposed solutions. In terms of cloud control applications, a visual feedback CCS was proposed in [27], using the powerful cloud computing to extract and analyze image features; the authors also analyzed the time-delay caused by the addition of cloud characteristics and proposed a switching gain control strategy for the influence of cloud characteristics. In [28], [29], a new virtual cloud laboratory education platform was proposed; it used a cloud storage platform to share learning materials and enable students to remotely control the virtual machine to perform experimental tasks. The intelligent transportation cyber-physical CCS was designed in [30], [31]. It can accurately predict short-term traffic flow and road congestion, and then obtain a real-time traffic flow control strategy through an intelligent optimal scheduling algorithm in the cloud. A cloud robot architecture was proposed in [32], enabling robots to share computing resources, information, and data with each other in the shared resource pool in the cloud, and to access new knowledge and skills. In [33], preliminary work of low-level motion control of a desktop 3D printer from the cloud was introduced. Through the cloud control algorithm provided by CaaS, the control performance of desktop 3D printer can be significantly improved at a low cost. Ultimately, the research and applications of the CCS are in preliminary stages. In [34], we proposed that the uncertainty of cloud computing would cause uncertainty of the cloud controller and affect the stability of the system, and used the Lyapunov stability theory [35]–[37] to design the controller to make the system stable. This paper focuses on the modeling and controller design of the discrete CCS with various uncertainties from the control point of view.

The contribution of this paper is mainly reflected in three aspects. First, we propose the basic framework of the CCS and the uncertainty decomposition strategy to simplify the modeling and controller design of the CCS. Second, the controller uncertainty is further elaborated and modeled according to the characteristics of the cloud control. Compared with the existing control system, it is a novel approach to controller design. Third, we propose a unified control system design framework with uncertainties including the controlled plant, network, and cloud controller; then, the corresponding mathematical model is established, and the controller is designed based on the stability principle.

The remainder of this paper is organized as follows. Section II presents a typical structure of the CCS and the uncertainty of CCS is analyzed and decomposed. Then in Section III, the model of uncertain CCS is given, considering the uncertainties existing in the controlled plant, network and cloud controller. In Section IV, the main results including stability analysis and controller parameter solution are presented. Section V conducts the CCS simulations for

two typical controlled plants, demonstrating the effectiveness and generalization of the proposed method, and Section VI concludes this paper.

Notations: Throughout this paper, R^n denotes n-dimensional Euclidean space, $R^{n\times m}$ is the set of all $n \times m$ real matrices, I denotes identity matrix of appropriate dimension, and "*" denotes the transposed matrices in the symmetric positions. The notations $X > Y$ and $X \geq Y$, where X and Y are matrices of the same dimensions, mean that the matrix $(X - Y)$ is positive definite and positive semi-definite, respectively. The interval matrix $[\underline{A}, \overline{A}]$ is defined as $[\underline{A}, \overline{A}] = \{A = [a_{ij}]; \underline{a}_{ij} \leq a_{ij} \leq \overline{a}_{ij}, 1 \leq i, j \leq n\}$, where $\underline{A} = [\underline{a}_{ij}]_{n\times n}$, $\overline{A} = [\overline{a}_{ij}]_{n\times n}$, and satisfies $\underline{a}_{ij} \leq \overline{a}_{ij}$. $\Pr\{\cdot\}$ means mathematical probability, $E\{\cdot\}$ stands for mathematical expectation and $Var\{\cdot\}$ denotes the variance.

II. TYPICAL STRUCTURE AND UNCERTAINY DECOMPOSITION OF THE CCS

In this section, first we introduce the basic concept and typical structure of CCS. Then, the uncertainties in the CCS are analyzed, and a decomposition strategy is proposed.

A. CLOUD CONTROL CONCEPT AND TYPICAL STRUCTURE

Reviewing the conventional control system design and the various control systems used, that is, from ICS, DCS, FCS to NCS, the software and hardware configuration are mainly around the core of "controller". The engineer's focus is the computer which runs various control algorithms, while the controlled plant (or process) is generally placed at the far end. However, the core idea based on cloud computing is to design the control system around the controlled plant (or process). Engineers can put various controllers (control algorithm, optimization algorithm, etc.) in the distant "cloud" to form a cloud controller [38], while the controlled plants only need to send the real-time detection signals and receive remote control signals through the highspeed network. The engineers can monitor the running status of the controlled plant in real time through a mobile device (such as a mobile phone) or a computer.

The CCS is structured as deep integration of cloud computing and a cyber-physical system. In [9], [14], a cloud-based automation architecture is proposed, which essentially relaxes the existing systems layers and reflects the relationship between each component and the layers in the industrial automation system. However, the CCS is an extension of the NCS and a new generation computer control system in the future. Therefore, we simplify and abstract the CCS as the basic structure of the computer control system from the control point of view, which divides the CCS into four parts, including controlled plant, network channel, cloud controller, and monitoring terminal as shown in Fig. 1. Compared with [9], [14], we can use the existing control theory to understand and analyze it more simply and easily.

The database, control algorithm library, optimized algorithm library, etc., are constructed on a cloud server, connected to each other and managed through server software

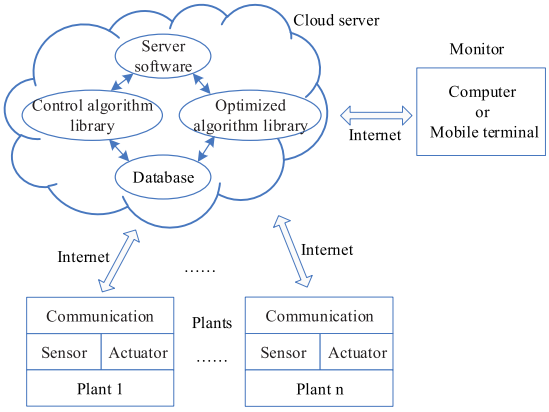

FIGURE 1. General structure of the CCS.

in the cloud. In the generalized controlled plant part, the top layer is the Internet communication interface, while the middle layer includes the sensor and actuator, and the bottom layer is the controlled plant itself. Each state variable of the bottom controlled plant is acquired by the sensor in real-time and sent to the cloud server; the actuator receives the control order from the cloud and then performs real-time control on each operating variable. For supervising the running state of the controlled plant in real-time, the monitor can be a mobile device terminal (such as a mobile phone) or a computer. The network is the Internet, connecting the cloud and the local controlled plants as well as the monitor and exchanging information among them.

This structure can effectively overcome problems such as the inflexible update and replacement of control algorithms and more requirements on system hardware, making the control system design more flexible and convenient. Without increasing the hardware cost, the cloud can identify the different characteristics of the controlled plant model according to a large amount of data about the controlled plant and the decision information obtained from big data mining in the cloud, so as to automatically select the appropriate control algorithm for engineers from the control algorithm library and optimization algorithm library. Engineers can also manually select the appropriate control algorithm or upload the control algorithm to the cloud according to the actual operation of the controlled plant in the industrial field; In this way, "customized" control is realized.

However, due to the uncertainties existing in the controlled plant, network channel, and cloud computing, the CCS is actually an uncertain system. The modeling and control of CCS are more complex and challenging due to the existence and high complexity of various uncertainties, compared with the previous control system. Next, we will analyze the uncertainties in CCS and decompose them.

B. UNCERTAINTY ANALYSIS OF CONTROLLED PLANT AND NETWORK

Due to the influence of internal parameter perturbation, parameter measurement error, identification error, and other

factors, the parameters of the actual controlled plant in the industry are often uncertain. In fact, we can say that most control systems are uncertain ones. Although uncertainty does not often change the system structure, its existence degrades the performance of the controller designed on the nominal system and can cause system instability. In most cases, the upper and lower bounds of parameters are easy to know, and therefore the interval number can be used to conveniently express the uncertain parameters of some control systems. In fact, considering the uncertainty of the controlled plant in the CCS, the designed controller will have a wider range of applications.

The cloud controller must communicate with the sensor and the actuator through the network, and the communication network has transmission time-delay, packet loss, timing disorder, and other uncertainties, due to congestion, equipment failure, network load [39], and other reasons, which will affect the performance and stability of the CCS. Besides, there are two different features in the network of the CCS. First, when modeling and controlling the control system, we must consider bilateral delay; however, in NCS, we can sometimes only consider the unilateral delay [40]–[42]. Even if the bilateral delay is considered in NCS [43]–[45], the network delay in CCS may show different characteristics due to the uncertainties of cloud computing itself. Second, due to the dynamic scheduling of resources, the uncertainty of cloud computing itself often leads to the time-related uncertainty of the cloud controller itself. This leads to the influence of the forward and feedback channel time-delays being different, and therefore, they cannot be simply combined into a single time-delay like in the NCS [46], [47].

C. CLOUD UNCERTAINTY ANALYSIS

As aforementioned, cloud computing also has many uncertainties due to dynamic resource scheduling [48], such as random computing delay, packet loss, and timing chaos. The existence of these uncertainties will cause the uncertainties of the cloud controller, among which the impact of time-delay on the cloud controller is most prominent.

The cloud controller is put in the cloud far away from the physical system, and due to load balancing, distributed computing, massive data processing, and other requirements, the data transmission delay between nodes and calculated delay of each node in the cloud [49] are larger than that of the NCS, and their randomness is more complex. At this time, the computing time-delay of the cloud controller cannot be simply included in the network time-delay, nor can it be ignored.

Although the reliability of the cloud is much greater than that of the network in general, it is inevitable that network congestion, connection interruptions, and channel interference will occur in the process of receiving and sending data packets, resulting in data packet loss. The communication information between nodes includes not only the data information required by the relevant calculation, but also the controller parameters, structure, control variables, and other information. Therefore, the packet loss at the cloud will not only cause the loss of the relevant sampling data, but also cause the loss of the relevant information of the controller, which is different from the packet loss at the network, resulting in the uncertainty of the controller itself.

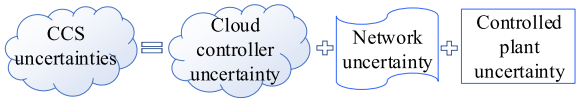

FIGURE 2. Uncertainties decomposition diagram of the CCS.

In addition, external attacks or interference may also cause cloud data to be leaked or tampered with artificially [50], which means the parameters and structure of various control algorithms placed in the cloud are changed, reducing the control effect without the cloud monitoring system noticing. This requires the cloud controller to have a certain degree of non-vulnerability so that the controller can hold the system stable when it is disturbed.

D. DECOMPOSITION STRATEGY OF CCS UNCERTAINTY

The CCS can be considered as the integration of cloud computing and the NCS, including all the characteristics of the NCS. The NCS itself has uncertainties of the network and the controlled plant. The CCS further increases the uncertainty by introducing cloud computing. The mixture of many uncertainties makes the modeling and control of the CCS more complex and difficult.

Therefore, in order to facilitate the analysis, this paper decomposes the uncertainties of the CCS, as shown in Fig. 2. It is considered that there are mainly three kinds of uncertainties in the generalized CCS: cloud controller uncertainty, network uncertainty, and controlled plant uncertainty, which together constitute the uncertainty of the whole system.

The advantage of this decomposition strategy is that it can make full use of the existing theoretical results of the NCS (including the network side and the controlled plant side) and concentrate on the uncertainty analysis of the cloud controller. On this basis, the three uncertainty models can be effectively combined according to some principles, thereby simplifying the complexity and reducing the difficulty of modeling the CCS with uncertainties.

III. CCS MODEL

In this section, the state-space model of a generalized uncertain controlled plant with the network delay and packet loss is established, and the cloud uncertainty is considered to obtain the cloud controller model including an observer with uncertain parameters and control law. Finally, the state equation of the closed-loop CCS is constructed based on these two models.

A. UNCERTAIN PARAMETERS SETTING

The structure of the discrete CCS considered in this paper is shown in Fig. 3. In the CCS, the time-delays of network channel and cloud controller are time-varying,

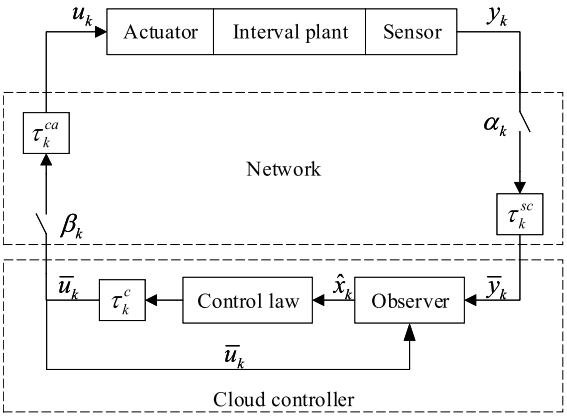

FIGURE 3. The structure of the discrete CCS with uncertainties.

so they are represented by three independent discrete Markov chains, here τ_k^{sc}, τ_k^{ca}, and τ_k^c respectively denote the feedback channel time-delay, forward channel time-delay, and cloud controller time-delay, which take values from $\Omega = \{0, \cdots, \tau_M^{sc}\}, \tilde{\Upsilon} = \{0, \cdots, \tau_M^{ca}\}$, $\Lambda = \{0, \cdots, \tau_M^c\}$, respectively. The transition probability matrices of τ_k^{sc}, τ_k^{ca}, and τ_k^c are $\Pi_{sc} = [\mu_{ab}], \Pi_{ca} = [\tilde{\sigma}_{ef}], \Pi_c = [\nu_{cd}]$, respectively, where $\mu_{ab}, \tilde{\sigma}_{ef}, \nu_{cd}$ are respectively defined as $\mu_{ab} = \Pr\{\mu_{k+1} = b \,|\mu_k = a\}$, $\tilde{\sigma}_{ef} = \Pr\{\tilde{\sigma}_{k+1} = f \,|\tilde{\sigma}_k = e\}$, $\nu_{cd} = \Pr\{\nu_{k+1} = d \,|\nu_k = c\}$, and $\mu_{ab} \geq 0, \tilde{\sigma}_{ef} \geq 0, \nu_{cd} \geq 0, \sum_{b=0}^{\tau_M^{sc}} \mu_{ab} = 1, \sum_{f=0}^{\tau_M^{ca}} \tilde{\sigma}_{ef} = 1, \sum_{d=0}^{\tau_M^c} \nu_{cd} = 1$. The sum of forward time-delay and controller time-delay $\tau_k^{ca}+\tau_k^c$ takes values from $\Upsilon = \{0, \cdots, \tau_M^{ca}+\tau_k^c\}$. The transition probability matrix is $\Pi_{ca+c} = [\sigma_{mn}]$, which can be obtained from the transition probability matrices of forward time-delay and controller time-delay, where σ_{mn} is defined as $\sigma_{mn} = \Pr\{\sigma_{k+1} = n \,|\sigma_k = m\}$, and $\sigma_{mn} \geq 0, \sum_{n=0}^{\tau_M^{ca}+\tau_M^c} \sigma_{mn} = 1$.

It is usually difficult to obtain all transition probability of the time-delay, so it is assumed that there are unknown elements in the transition probability matrix. For notational clarity, $\forall b \in \Omega$, let $\Omega = \Omega_k^a + \Omega_{uk}^a$, with $\Omega_k^a = \{b : \mu_{ab} \, is \, known\}, \Omega_{uk}^a = \{b : \mu_{ab} \, is \, unknown\}$. If Ω_k^a is not an empty set, it can be further represented as $\Omega_k^a = \{\Omega_1^a, \Omega_2^a \cdots, \Omega_p^a\}$, where Ω_p^a represents the subscript of the pth known element of the ath row of the matrix Π_{sc}. Ω_{uk}^a can be described as $\Omega_{uk}^a = \{\Omega_{u1}^a, \Omega_{u2}^a \cdots, \Omega_{u(M-p)}^a\}$, where $\Omega_{u(M-p)}^a$ represents the subscript of the $(M-p)$th unknown element in the ath row of matrix Π_{sc}.

Similarly, $\forall d \in \Lambda$, let $\Lambda = \Lambda_k^c + \Lambda_{uk}^c$, with $\Lambda_k^c = \{d : \nu_{cd} \, is \, known\}, \Lambda_{uk}^c = \{d : \nu_{cd} \, is \, unknown\}$. If Λ_k^c is not an empty set, it can be further represented as $\Lambda_k^c = \{\Lambda_1^c, \Lambda_2^c \cdots, \Lambda_r^c\}$, where Λ_r^c represents the subscript of the rth known element of the cth row of the matrix Π_c. Λ_{uk}^c can be described as $\Lambda_{uk}^c = \{\Lambda_{u1}^c, \Lambda_{u2}^c \cdots, \Lambda_{u(M-r)}^c\}$, where $\Lambda_{u(M-r)}^c$ represents the subscript of the $(M-r)$th unknown element in the cth row of matrix Π_c. $\forall m \in \Upsilon$, let $\Upsilon = \Upsilon_k^m + \Upsilon_{uk}^m$, with $\Upsilon_k^m = \{n : \sigma_{mn} \, is \, known\}, \Upsilon_{uk}^m = \{n : \sigma_{mn} \, is \, unknown\}$. If Υ_k^m is not an empty set, it can be further represented as $\Upsilon_k^m = \{\Upsilon_1^m, \Upsilon_2^m, \cdots, \Upsilon_t^m\}$, where Υ_t^m represents the subscript of the tth known element of the mth row of the matrix Π_{ca+c}. Υ_{uk}^m can be described as $\Upsilon_{uk}^m = \{\Upsilon_{u1}^m, \Upsilon_{u2}^m \cdots, \Upsilon_{u(M-t)}^m\}$, where $\Upsilon_{u(M-t)}^m$ represents the subscript of the $(M-t)$th unknown element in the mth row of matrix Π_{ca+c}.

In Fig. 3, when the switch of the feedback channel or the forward channel is closed, it indicates that the data packet of the corresponding channel is successfully transmitted; otherwise, the packet loss occurs. Therefore, independent random variables α_k, β_k are used to represent packet loss of feedback and forward channel, respectively, which obey Bernoulli distribution. When the value of the random variable takes 1, it means that the data packet is successfully transmitted; otherwise, packet loss occurs. Random variables satisfy the following characteristics

$$\Pr\{\alpha_k = 1\} = E\{\alpha_k\} \triangleq \bar{\alpha}, \tag{1a}$$
$$\Pr\{\alpha_k = 0\} \triangleq 1 - \bar{\alpha}, \tag{1b}$$
$$Var\{\alpha_k\} = E\{(\alpha_k - \bar{\alpha})^2\} = (1-\bar{\alpha})\bar{\alpha} \triangleq \alpha_1^2, \tag{1c}$$
$$\Pr\{\beta_k = 1\} = E\{\beta_k\} \triangleq \bar{\beta}, \tag{1d}$$
$$\Pr\{\beta_k = 0\} \triangleq 1 - \bar{\beta}, \tag{1e}$$
$$Var\{\beta_k\} = E\{(\beta_k - \bar{\beta})^2\} = (1-\bar{\beta})\bar{\beta} \triangleq \beta_1^2, \tag{1f}$$
$$E\{(\beta_k - \bar{\beta})\} = E(\beta_k) - \bar{\beta} = \bar{\beta} - \bar{\beta} = 0, \tag{1g}$$
$$E\{(\alpha_k - \bar{\alpha})\} = 0. \tag{1h}$$

B. STATE EQUATION OF THE CLOSED-LOOP CCS

The state-space model of the discrete controlled plant is

$$\begin{cases} x_{k+1} = A_1 x_k + B_1 u_k \\ y_k = C x_k, \end{cases} \tag{2}$$

where $x_k \in R^n, u_k \in R^m, y_k \in R^p$ are the state, input, and output vectors, respectively. $A_1 \in R^{n\times n}$ and $B_1 \in R^{n\times m}$ are the interval parameter matrices with the appropriate dimensions, that is, $A_1 = [\underline{A}_1, \overline{A}_1], B_1 = [\underline{B}_1, \overline{B}_1]$, and $C \in R^{p\times n}$ is a constant matrix with the appropriate dimension. According to relevant theories of interval analysis [51], it can be obtained that

$$A_0 = \frac{1}{2}(\underline{A}_1 + \overline{A}_1), \tag{3a}$$
$$B_0 = \frac{1}{2}(\underline{B}_1 + \overline{B}_1), \tag{3b}$$
$$\Delta A_1 = \frac{1}{2}(\overline{A}_1 - \underline{A}_1) = (a_{1,ij}^*)_{n\times n}, \tag{3c}$$
$$\Delta B_1 = \frac{1}{2}(\overline{B}_1 - \underline{B}_1) = (b_{1,ik}^*)_{n\times m}, \tag{3d}$$

where A_0 and B_0 are the system matrix and input matrix of the nominal system, respectively. Then, A_1 and B_1 can be written as $A_1 = A_0 + D_1 F_1 E_1, B_1 = B_0 + D_2 F_2 E_2$, where

$$D_1 = [a_{1,11}^* I_1, \cdots, a_{1,1n}^* I_1, \cdots, a_{1,n1}^* I_n, \cdots, a_{1,nn}^* I_n]_{n\times n^2}, \tag{4a}$$

$$E_1 = [I_1, \cdots, I_n, \cdots, I_1, \cdots, I_n]^T_{n^2\times n}, \tag{4b}$$

$$D_2 = [b^*_{1,11}I_1, \cdots, b^*_{1,1m}I_1, \cdots, b^*_{1,n1}I_n, \cdots, b^*_{1,nm}I_n]_{n\times nm}, \tag{4c}$$

$$E_2 = [I_1, \cdots, I_n, \cdots, I_1, \cdots, I_n]^T_{nm\times n}, \tag{4d}$$

where I_i denotes the ith column vector of the identity matrix, and F_1 and F_2 are the time-varying diagonal matrices with appropriate dimensions, and the absolute values of their diagonal elements are not larger than 1.

In the control system, all or part of the state cannot be directly measured, and the state observer can be described as

$$\begin{cases} \hat{x}_{k+1} = A_2\hat{x}_k + B_2\bar{u}_k + L\left(\bar{y}_k - \alpha_k\hat{y}_{k-\tau^{sc}_k}\right) \\ \hat{y}_k = C\hat{x}_k, \end{cases} \tag{5}$$

where $\hat{x}_k$ is the state vector of the observer, $\hat{y}_k$ is the output vector of the observer, L is the observer gain matrix, $\bar{y}_k$ and $\bar{u}_k$ are system output and control input vectors sent to the observer, respectively. $\alpha_k\hat{y}_{k-\tau^{sc}_k}$ is the output value of the observer corresponding to $\bar{y}_k$, which is used to correct the state reconstruction. In addition to time-delay, other uncertain factors, such as packet loss and external disturbance in cloud computing, may change the parameters of cloud controller. Therefore, it is assumed that $A_2 \in R^{n\times n}$, $B_2 \in R^{n\times m}$ are the interval parameter matrices with the appropriate dimensions, whose median values are the same as that of the nominal system, but the widths are different, that is, $A_2 = [\underline{A}_2, \overline{A}_2]$, $B_2 = [\underline{B}_2, \overline{B}_2]$. Similarly, it can be obtained that

$$A_0 = \frac{1}{2}(\underline{A}_2 + \overline{A}_2) = \frac{1}{2}(\underline{A}_1 + \overline{A}_1), \tag{6a}$$

$$B_0 = \frac{1}{2}(\underline{B}_2 + \overline{B}_2) = \frac{1}{2}(\underline{B}_1 + \overline{B}_1), \tag{6b}$$

$$\Delta A_2 = \frac{1}{2}(\overline{A}_2 - \underline{A}_2) = (a^*_{2,ij})_{n\times n}, \tag{6c}$$

$$\Delta B_2 = \frac{1}{2}(\overline{B}_2 - \underline{B}_2) = (b^*_{2,ik})_{n\times m}. \tag{6d}$$

Then, A_2 and B_2 can be written as $A_2 = A_0 + D_3F_3E_3$, $B_2 = B_0 + D_4F_4E_4$, where

$$D_3 = [a^*_{2,11}I_1, \cdots, a^*_{2,1n}I_1, \cdots, a^*_{2,n1}I_n, \cdots, a^*_{2,nn}I_n]_{n\times n^2}, \tag{7a}$$

$$E_3 = [I_1, \cdots, I_n, \cdots, I_1, \cdots, I_n]^T_{n^2\times n}, \tag{7b}$$

$$D_4 = [b^*_{2,11}I_1, \cdots, b^*_{2,1m}I_1, \cdots, b^*_{2,n1}I_n, \cdots, b^*_{2,nm}I_n]_{n\times nm}, \tag{7c}$$

$$E_4 = [I_1, \cdots, I_n, \cdots, I_1, \cdots, I_n]^T_{nm\times n}, \tag{7d}$$

where I_i denotes the ith column vector of the identity matrix, and F_3 and F_4 are the time-varying diagonal matrices with appropriate dimensions, and the absolute values of their diagonal elements are not larger than 1.

The output of the controller considering the time-delay of the cloud controller can be expressed as

$$\bar{u}_k = K\hat{x}_{k-\tau^c_k} \tag{8}$$

where K is the gain matrix of the control law.

Considering network time-delay and packet loss, the system output sent to observer and control input received by actuator can be expressed as

$$\bar{y} = \alpha_k y_{k-\tau^{sc}_k}, \tag{9}$$

$$u_k = \beta_k\bar{u}_{k-\tau^{ca}_k} = \beta_k K\hat{x}_{k-\tau^{ca}_k-\tau^c_k}. \tag{10}$$

State estimation error and augmented matrix are respectively defined as

$$e_k = x_k - \hat{x}_k, \tag{11}$$

$$\xi_k = \left[x_k^T\, e_k^T\right]^T. \tag{12}$$

The state equation of the closed-loop CCS can be obtained from (2) - (12).

$$\xi_{k+1} = \tilde{A}\xi_k + \alpha_k I_1 L\tilde{C}\xi_{k-\phi_k} + \tilde{B}KI_2\xi_{k-\varphi_k} + \beta_k\hat{B}KI_3\xi_{k-\psi_k} \tag{13}$$

where $\tilde{A} = \begin{bmatrix} A_1 & 0 \\ A_1 - A_2 & A_2 \end{bmatrix}$, $I_1 = \begin{bmatrix} 0 \\ I \end{bmatrix}$, $\tilde{C} = \begin{bmatrix} 0 & -C \end{bmatrix}$, $\tilde{B} = \begin{bmatrix} 0 \\ B_2 \end{bmatrix}$, $I_2 = \begin{bmatrix} -I & I \end{bmatrix}$, $\hat{B} = \begin{bmatrix} B_1 \\ B_1 \end{bmatrix}$, $I_3 = \begin{bmatrix} I & -I \end{bmatrix}$, $\phi_k = \tau^{sc}_k$, $\varphi_k = \tau^c_k$, $\psi_k = \tau^{ca}_k + \tau^c_k$.

Because A_1, B_1, A_2, and B_2 are interval matrices, $\tilde{A}$, $\tilde{B}$, and $\hat{B}$ can be expressed as

$$\begin{aligned} &\tilde{A} = \tilde{A}_0 + \tilde{D}_1\tilde{F}_1\tilde{E}_1, \quad \tilde{B} = \tilde{B}_0 + \tilde{D}_2\tilde{F}_2\tilde{E}_2, \\ &\hat{B} = \hat{B}_0 + \tilde{D}_3\tilde{F}_3\tilde{E}_3, \end{aligned} \tag{14}$$

where $\tilde{A}_0 = \begin{bmatrix} A_0 & 0 \\ 0 & A_0 \end{bmatrix}$, $\tilde{D}_1 = \begin{bmatrix} D_1 & 0 \\ D_1 & D_3 \end{bmatrix}$, $\tilde{F}_1 = \begin{bmatrix} F_1 & 0 \\ 0 & F_3 \end{bmatrix}$, $\tilde{E}_1 = \begin{bmatrix} E_1 & 0 \\ -E_3 & E_3 \end{bmatrix}$, $\tilde{B}_0 = \begin{bmatrix} 0 \\ B_0 \end{bmatrix}$, $\tilde{D}_2 = \begin{bmatrix} 0 \\ D_4 \end{bmatrix}$, $\tilde{F}_2 = F_4$, $\tilde{E}_2 = E_4$, $\hat{B}_0 = \begin{bmatrix} B_0 \\ B_0 \end{bmatrix}$, $\tilde{D}_3 = \begin{bmatrix} D_2 \\ D_2 \end{bmatrix}$, $\tilde{F}_3 = F_2$, $\tilde{E}_3 = E_2$.

IV. MAIN RESULTS

In this section, the main results of this paper are presented. Firstly, the following definitions and lemmas are given. Then, the theorem about the stability criteria of the CCS is given on the basis of the Lyapunov theorem. And the linear matrix inequality (LMI) method is adopted to obtain the parameters of the cloud controller.

A. RELATED DEFINITIONS AND LEMMAS

Definition 1 ([52]): For any initial system state ξ_0 and initial time-delay mode $\phi_0 \in \Omega, \varphi_0 \in \Lambda, \psi_0 \in \Upsilon$, if there exists a positive definite matrix W, such that

$$E\left\{\sum_{k=0}^{\infty}\|\xi_k\|^2\big|_{\phi_0,\varphi_0,\psi_0}\right\} < \xi_0^T W\xi_0 \tag{15}$$

the closed-loop system (13) is said to be stochastically stable.

Lemma 1 ([53]): For any positive definite matrix H and two scalar θ, θ_0 satisfying $\theta > \theta_0 \geq 1$, the following formula always holds:

$$\left(\sum_{\rho=\theta_0}^{\theta}\nu_\rho\right)^T H\sum_{\rho=\theta_0}^{\theta}\nu_\rho \leq (\theta - \theta_0 + 1)\sum_{\rho=\theta_0}^{\theta}\nu_\rho^T H\nu_\rho \tag{16}$$

Lemma 2 ([54]): Given real matrices $M = M^T$, H and E with $F(t)$ satisfying $F(t)F^T(t) < I$, then $M + HFE + E^TF^TH^T < 0$, if and only if there exists a positive scalar ε such that

$$M + \varepsilon HH^T + \varepsilon^{-1}E^TE < 0 \tag{17}$$

or equivalently

$$\begin{bmatrix} M & \varepsilon H & E^T \\ \varepsilon H^T & -\varepsilon I & 0 \\ E & 0 & -\varepsilon I \end{bmatrix} < 0 \tag{18}$$

B. STABILITY ANALYSIS

In this subsection, a stability theorem will be stated, which gives a sufficient condition for the stochastic stability of the closed-loop uncertain CCS.

Theorem 1: Under the presented control law (8), the CCS (13) with uncertainties is stochastically stable if for given scalars $0 \le \bar{\alpha} \le 1, 0 \le \bar{\beta} \le 1$, there exist matrices K, L with proper dimensions and symmetric positive definite matrices $R_{acm} > 0, R_{bdn} > 0, P_1 > 0, P_2 > 0, P_3 > 0, P_4 > 0, P_5 > 0, P_6 > 0, Q_1 > 0, Q_2 > 0, Q_3 > 0$, such that the following matrix inequality (19) holds for all $a, b \in \Omega, c, d \in \Lambda, m, n \in \Upsilon$.

$$\Gamma \triangleq \begin{bmatrix} \Gamma_{11} & * & * & * & * & * & * \\ \Gamma_{21} & \Gamma_{22} & * & * & * & * & * \\ \Gamma_{31} & \Gamma_{32} & \Gamma_{33} & * & * & * & * \\ \Gamma_{41} & \Gamma_{42} & \Gamma_{43} & \Gamma_{44} & * & * & * \\ 0 & Q_1 & 0 & 0 & -P_1-Q_1 & * & * \\ 0 & 0 & Q_2 & 0 & 0 & -P_2-Q_2 & * \\ 0 & 0 & 0 & Q_3 & 0 & 0 & -P_3-Q_3 \end{bmatrix} < 0 \tag{19}$$

where

$$\begin{aligned}
\Gamma_{11} &= \tilde{A}^T\bar{R}_{bdn}\tilde{A} - R_{acm} + P_1 + P_2 + P_3 + (\phi_M + 2)P_4 \\
&\quad + (\varphi_M + 2)P_5 + (\psi_M + 2)P_6 + \phi_M^2(\tilde{A}-I)^TQ_1(\tilde{A}-I) \\
&\quad + \varphi_M^2(\tilde{A}-I)^TQ_2(\tilde{A}-I) + \psi_M^2(\tilde{A}-I)^TQ_3(\tilde{A}-I) \\
&\quad - Q_1 - Q_2 - Q_3 \\
\Gamma_{21} &= (\bar{\alpha}I_1L\tilde{C})^T\bar{R}_{bdn}\tilde{A} + \phi_M^2(\bar{\alpha}I_1L\tilde{C})^TQ_1(\tilde{A}-I) \\
&\quad + \varphi_M^2(\bar{\alpha}I_1L\tilde{C})^TQ_2(\tilde{A}-I) \\
&\quad + \psi_M^2(\bar{\alpha}I_1L\tilde{C})^TQ_3(\tilde{A}-I) + Q_1 \\
\Gamma_{22} &= (\alpha_1^2 + \bar{\alpha}^2)(I_1L\tilde{C})^T\bar{R}_{bdn}I_1L\tilde{C} \\
&\quad - P_4 + \phi_M^2(\alpha_1^2 + \bar{\alpha}^2)(I_1L\tilde{C})^TQ_1I_1L\tilde{C} \\
&\quad + \varphi_M^2(\alpha_1^2 + \bar{\alpha}^2)(I_1L\tilde{C})^TQ_2I_1L\tilde{C} \\
&\quad + \psi_M^2(\alpha_1^2 + \bar{\alpha}^2)(I_1L\tilde{C})^TQ_3I_1L\tilde{C} - 2Q_1 \\
\Gamma_{31} &= (\tilde{B}KI_2)^T\bar{R}_{bdn}\tilde{A} + \phi_M^2(\tilde{B}KI_2)^TQ_1(\tilde{A}-I) \\
&\quad + \varphi_M^2(\tilde{B}KI_2)^TQ_2(\tilde{A}-I) \\
&\quad + \psi_M^2(\tilde{B}KI_2)^TQ_3(\tilde{A}-I) + Q_2 \\
\Gamma_{32} &= (\tilde{B}KI_2)^T\bar{R}_{bdn}\bar{\alpha}I_1L\tilde{C} + \phi_M^2(\tilde{B}KI_2)^TQ_1\bar{\alpha}I_1L\tilde{C} \\
&\quad + \varphi_M^2(\tilde{B}KI_2)^TQ_2\bar{\alpha}I_1L\tilde{C} + \psi_M^2(\tilde{B}KI_2)^TQ_3\bar{\alpha}I_1L\tilde{C} \\
\Gamma_{33} &= (\tilde{B}KI_2)^T\bar{R}_{bdn}\tilde{B}KI_2 - P_5 + \phi_M^2(\tilde{B}KI_2)^TQ_1\tilde{B}KI_2 \\
&\quad + \varphi_M^2(\tilde{B}KI_2)^TQ_2\tilde{B}KI_2 + \psi_M^2(\tilde{B}KI_2)^TQ_3\tilde{B}KI_2 - 2Q_2 \\
\Gamma_{41} &= (\bar{\beta}\hat{B}KI_3)^T\bar{R}_{bdn}\tilde{A} + \phi_M^2(\bar{\beta}\hat{B}KI_3)^TQ_1(\tilde{A}-I) \\
&\quad + \varphi_M^2(\bar{\beta}\hat{B}KI_3)^TQ_2(\tilde{A}-I) \\
&\quad + \psi_M^2(\bar{\beta}\hat{B}KI_3)^TQ_3(\tilde{A}-I) + Q_3 \\
\Gamma_{42} &= (\bar{\beta}\hat{B}KI_3)^T\bar{R}_{bdn}\bar{\alpha}I_1L\tilde{C} \\
&\quad + \phi_M^2(\bar{\beta}\hat{B}KI_3)^TQ_1\bar{\alpha}I_1L\tilde{C} \\
&\quad + \varphi_M^2(\bar{\beta}\hat{B}KI_3)^TQ_2\bar{\alpha}I_1L\tilde{C} \\
&\quad + \psi_M^2(\bar{\beta}\hat{B}KI_3)^TQ_3\bar{\alpha}I_1L\tilde{C} \\
\Gamma_{43} &= (\bar{\beta}\hat{B}KI_3)^T\bar{R}_{bdn}\tilde{B}KI_2 + \phi_M^2(\bar{\beta}\hat{B}KI_3)^TQ_1\tilde{B}KI_2 \\
&\quad + \varphi_M^2(\bar{\beta}\hat{B}KI_3)^TQ_2\tilde{B}KI_2 + \psi_M^2(\bar{\beta}\hat{B}KI_3)^TQ_3\tilde{B}KI_2 \\
\Gamma_{44} &= (\beta_1^2 + \bar{\beta}^2)(\hat{B}KI_3)^T\bar{R}_{bdn}\hat{B}KI_3 - P_6 \\
&\quad + \phi_M^2(\beta_1^2 + \bar{\beta}^2)(\hat{B}KI_3)^TQ_1\hat{B}KI_3 \\
&\quad + \varphi_M^2(\beta_1^2 + \bar{\beta}^2)(\hat{B}KI_3)^TQ_2\hat{B}KI_3 \\
&\quad + \psi_M^2(\beta_1^2 + \bar{\beta}^2)(\hat{B}KI_3)^TQ_3\hat{B}KI_3 - 2Q_3 \\
\bar{R}_{bdn} &= \sum_{b=0}^{\phi_M}\sum_{d=0}^{\varphi_M}\sum_{n=0}^{\psi_M}\mu_{ab}\nu_{cd}\sigma_{mn}R_{bdn}.
\end{aligned}$$

Proof: As shown in Appendix A.

C. SOLUTION OF CONTROLLER PARAMETERS

The matrix inequality in (19) is bilinear, which needs to be converted into LMI to obtain the control law gain matrix K and the observer gain matrix L, thus, Theorem 2 is given.

Theorem 2: Under the presented control law (8), the CCS (13) with uncertainties is stochastically stable if for given scalars $0 \le \bar{\alpha} \le 1, 0 \le \bar{\beta} \le 1$, there exist matrices K, L with proper dimensions, symmetric matrices $R_{acm} > 0, S_{bdn} > 0, P_1 > 0, P_2 > 0, P_3 > 0, P_4 > 0, P_5 > 0, P_6 > 0, Q_1 > 0, Q_2 > 0, Q_3 > 0$ and real scalars $\varepsilon_1, \varepsilon_2, \varepsilon_3, \varepsilon_4, \varepsilon_5, \varepsilon_6, \varepsilon_7, \varepsilon_8 > 0$, such that the following linear matrix inequality (30) - (37) hold for all $a, b \in \Omega, c, d \in \Lambda, m, n \in \Upsilon$.

$$\begin{bmatrix} \mu\nu\sigma\Xi_0 & * & * & * & * & * \\ X_{\Omega_k^a\Lambda_k^c\Upsilon_k^m} & \Psi_{\Omega_k^a\Lambda_k^c\Upsilon_k^m} & * & * & * & * \\ \varepsilon_1\tilde{D}^T & 0 & -\varepsilon_1 I & * & * & * \\ 0 & \varepsilon_1\tilde{D}^T_{\Omega_k^a\Lambda_k^c\Upsilon_k^m} & 0 & -\varepsilon_1 I & * & * \\ \tilde{E} & 0 & 0 & 0 & -\varepsilon_1 I & * \\ \tilde{E}_{\Omega_k^a\Lambda_k^c\Upsilon_k^m} & 0 & 0 & 0 & 0 & -\varepsilon_1 I \end{bmatrix} < 0 \tag{30}$$

$$\begin{bmatrix} \mu\sigma\Xi_0 & * & * & * & * & * \\ X_{\Omega_k^a\Lambda_{uk}^c\Upsilon_k^m} & \Psi_{\Omega_k^a\Lambda_{uk}^c\Upsilon_k^m} & * & * & * & * \\ \varepsilon_2\tilde{D}^T & 0 & -\varepsilon_2 I & * & * & * \\ 0 & \varepsilon_2\tilde{D}^T_{\Omega_k^a\Lambda_{uk}^c\Upsilon_k^m} & 0 & -\varepsilon_2 I & * & * \\ \tilde{E} & 0 & 0 & 0 & -\varepsilon_2 I & * \\ \tilde{E}_{\Omega_k^a\Lambda_{uk}^c\Upsilon_k^m} & 0 & 0 & 0 & 0 & -\varepsilon_2 I \end{bmatrix} < 0 \tag{31}$$
$\forall d \in \Lambda_{uk}^c$

$$\begin{bmatrix} \mu\nu\Xi_0 & * & * & * & * & * \\ X_{\Omega_k^a\Lambda_k^c\Upsilon_{uk}^m} & \Psi_{\Omega_k^a\Lambda_k^c\Upsilon_{uk}^m} & * & * & * & * \\ \varepsilon_3\tilde{D}^T & 0 & -\varepsilon_3 I & * & * & * \\ 0 & \varepsilon_3\tilde{D}^T_{\Omega_k^a\Lambda_k^c\Upsilon_{uk}^m} & 0 & -\varepsilon_3 I & * & * \\ \tilde{E} & 0 & 0 & 0 & -\varepsilon_3 I & * \\ \tilde{E}_{\Omega_k^a\Lambda_k^c\Upsilon_{uk}^m} & 0 & 0 & 0 & 0 & -\varepsilon_3 I \end{bmatrix} < 0$$
$$\forall n \in \Upsilon_{uk}^m \tag{32}$$

$$\begin{bmatrix} \mu\Xi_0 & * & * & * & * & * \\ X_{\Omega_k^a\Lambda_{uk}^c\Upsilon_{uk}^m} & \Psi_{\Omega_k^a\Lambda_{uk}^c\Upsilon_{uk}^m} & * & * & * & * \\ \varepsilon_4\tilde{D}^T & 0 & -\varepsilon_4 I & * & * & * \\ 0 & \varepsilon_4\tilde{D}^T_{\Omega_k^a\Lambda_{uk}^c\Upsilon_{uk}^m} & 0 & -\varepsilon_4 I & * & * \\ \tilde{E} & 0 & 0 & 0 & -\varepsilon_4 I & * \\ \tilde{E}_{\Omega_k^a\Lambda_{uk}^c\Upsilon_{uk}^m} & 0 & 0 & 0 & 0 & -\varepsilon_4 I \end{bmatrix} < 0$$
$$\forall d \in \Lambda_{uk}^c, \quad \forall n \in \Upsilon_{uk}^m \tag{33}$$

$$\begin{bmatrix} \nu\sigma\Xi_0 & * & * & * & * & * \\ X_{\Omega_{uk}^a\Lambda_k^c\Upsilon_k^m} & \Psi_{\Omega_{uk}^a\Lambda_k^c\Upsilon_k^m} & * & * & * & * \\ \varepsilon_5\tilde{D}^T & 0 & -\varepsilon_5 I & * & * & * \\ 0 & \varepsilon_5\tilde{D}^T_{\Omega_{uk}^a\Lambda_k^c\Upsilon_k^m} & 0 & -\varepsilon_5 I & * & * \\ \tilde{E} & 0 & 0 & 0 & -\varepsilon_5 I & * \\ \tilde{E}_{\Omega_{uk}^a\Lambda_k^c\Upsilon_k^m} & 0 & 0 & 0 & 0 & -\varepsilon_5 I \end{bmatrix} < 0$$
$$\forall b \in \Omega_{uk}^a \tag{34}$$

$$\begin{bmatrix} \nu\Xi_0 & * & * & * & * & * \\ X_{\Omega_{uk}^a\Lambda_k^c\Upsilon_{uk}^m} & \Psi_{\Omega_{uk}^a\Lambda_k^c\Upsilon_{uk}^m} & * & * & * & * \\ \varepsilon_6\tilde{D}^T & 0 & -\varepsilon_6 I & * & * & * \\ 0 & \varepsilon_6\tilde{D}^T_{\Omega_{uk}^a\Lambda_k^c\Upsilon_{uk}^m} & 0 & -\varepsilon_6 I & * & * \\ \tilde{E} & 0 & 0 & 0 & -\varepsilon_6 I & * \\ \tilde{E}_{\Omega_{uk}^a\Lambda_k^c\Upsilon_{uk}^m} & 0 & 0 & 0 & 0 & -\varepsilon_6 I \end{bmatrix} < 0$$
$$\forall b \in \Omega_{uk}^a, \quad \forall n \in \Upsilon_{uk}^m \tag{35}$$

$$\begin{bmatrix} \sigma\Xi_0 & * & * & * & * & * \\ X_{\Omega_{uk}^a\Lambda_{uk}^c\Upsilon_k^m}\Psi_{\Omega_{uk}^a\Lambda_{uk}^c\Upsilon_k^m} & * & * & * & * \\ \varepsilon_7\tilde{D}^T & 0 & -\varepsilon_7 I & * & * & * \\ 0 & \varepsilon_7\tilde{D}^T_{\Omega_{uk}^a\Lambda_{uk}^c\Upsilon_k^m} & 0 & -\varepsilon_7 I & * & * \\ \tilde{E} & 0 & 0 & 0 & -\varepsilon_7 I & * \\ \tilde{E}_{\Omega_{uk}^a\Lambda_{uk}^c\Upsilon_k^m} & 0 & 0 & 0 & 0 & -\varepsilon_7 I \end{bmatrix} < 0$$
$$\forall b \in \Omega_{uk}^a, \quad \forall d \in \Lambda_{uk}^c \tag{36}$$

$$\begin{bmatrix} \Xi_0 & * & * & * & * & * \\ X_{\Omega_{uk}^a\Lambda_{uk}^c\Upsilon_{uk}^m}\Psi_{\Omega_{uk}^a\Lambda_{uk}^c\Upsilon_{uk}^m} & * & * & * & * \\ \varepsilon_8\tilde{D}^T & 0 & -\varepsilon_8 I & * & * & * \\ 0 & \varepsilon_8\tilde{D}^T_{\Omega_{uk}^a\Lambda_{uk}^c\Upsilon_{uk}^m} & 0 & -\varepsilon_8 I & * & * \\ \tilde{E} & 0 & 0 & 0 & -\varepsilon_8 I & * \\ \tilde{E}_{\Omega_{uk}^a\Lambda_{uk}^c\Upsilon_{uk}^m} & 0 & 0 & 0 & 0 & -\varepsilon_8 I \end{bmatrix} < 0$$
$$\forall b \in \Omega_{uk}^a, \quad \forall d \in \Lambda_{uk}^c, \ \forall n \in \Upsilon_{uk}^m \tag{37}$$

where the definition of parameters in (30)-(37) is given in Appendix B.

Proof: Equation (19) can be converted to (38).

$$\Gamma = \Xi_{11} - \Xi_{21}^T\Xi_{22}^{-1}\Xi_{21} - \Xi_{31}^T\Xi_{33}^{-1}\Xi_{31} - \Xi_{41}^T\Xi_{44}^{-1}\Xi_{41} - X^T\Psi^{-1}X < 0 \tag{38}$$

where

$$\Xi_{11} = \begin{bmatrix} \tilde{\Xi}_{11} & * & * & * & * & * & * \\ Q_1 - P_4 - 2Q_1 & * & * & * & * & * & * \\ Q_2 & 0 & -P_5 - 2Q_2 & * & * & * & * \\ Q_3 & 0 & 0 & -P_6 - 2Q_3 & * & * & * \\ 0 & Q_1 & 0 & 0 & -P_1 - Q_1 & * & * \\ 0 & 0 & Q_2 & 0 & 0 & -P_2 - Q_2 & * \\ 0 & 0 & 0 & Q_3 & 0 & 0 & -P_3 - Q_3 \end{bmatrix},$$
$$\tilde{\Xi}_{11} = -R_{acm} + P_1 + P_2 + P_3 + (\phi_M + 2)P_4 + (\varphi_M + 2)P_5 + (\psi_M + 2)P_6 - Q_1 - Q_2 - Q_3,$$
$$\Xi_{21} = \phi_M \mathrm{X}, \quad \Xi_{31} = \varphi_M \mathrm{X}, \ \Xi_{41} = \psi_M \mathrm{X},$$
$$\Xi_{22} = diag\{-Q_1^{-1} - Q_1^{-1} - Q_1^{-1}\},$$
$$\Xi_{33} = diag\{-Q_2^{-1} - Q_2^{-1} - Q_2^{-1}\},$$
$$\Xi_{44} = diag\{-Q_3^{-1} - Q_3^{-1} - Q_3^{-1}\}, \ \Psi = diag\{-\bar{R}_{bdn}^{-1} \cdots - \bar{R}_{bdn}^{-1}\},$$
$$\mathrm{X} = \begin{bmatrix} (\tilde{A} - I) & \bar{\alpha} I_1 L\tilde{C} & \tilde{B}KI_2 & \bar{\beta}\hat{B}KI_3 & 0\ 0\ 0 \\ 0 & \alpha_1 I_1 L\tilde{C} & 0 & 0 & 0\ 0\ 0 \\ 0 & 0 & 0 & \beta_1\hat{B}KI_3 & 0\ 0\ 0 \end{bmatrix}.$$

By using the Schur Complement, (38) can be written as (39).

$$\begin{aligned} \Gamma &= \Xi + \bar{\eta}_1^T\bar{R}_{bdn}\bar{\eta}_1 + \bar{\eta}_2^T\bar{R}_{bdn}\bar{\eta}_2 + \bar{\eta}_3^T\bar{R}_{bdn}\bar{\eta}_3 \\ &= (\mu\nu\sigma + \mu\nu\bar{\sigma} + \mu\bar{\nu}\sigma + \mu\bar{\nu}\bar{\sigma} + \bar{\mu}\nu\sigma + \bar{\mu}\nu\bar{\sigma} + \bar{\mu}\bar{\nu}\sigma + \bar{\mu}\bar{\nu}\bar{\sigma})\Xi \\ &\quad + \bar{\eta}_1^T\bar{R}_{bdn}\bar{\eta}_1 + \bar{\eta}_2^T\bar{R}_{bdn}\bar{\eta}_2 + \bar{\eta}_3^T\bar{R}_{bdn}\bar{\eta}_3 \\ &= \mu\nu\sigma\,\tilde{\Xi} + \bar{\nu}(\mu\sigma\,\tilde{\Xi}) + \bar{\sigma}(\mu\nu\,\tilde{\Xi}) + \bar{\nu}\bar{\sigma}(\mu\,\tilde{\Xi}) + \bar{\mu}(\nu\sigma\,\tilde{\Xi}) \\ &\quad + \bar{\mu}\bar{\sigma}(\nu\,\tilde{\Xi}) + \bar{\mu}\bar{\nu}(\sigma\,\tilde{\Xi}) + \bar{\mu}\bar{\nu}\bar{\sigma}\,\tilde{\Xi} < 0 \end{aligned} \tag{39}$$

where

$$\tilde{\Xi} = \Xi + \bar{\eta}_1^T R_{bdn}\bar{\eta}_1 + \bar{\eta}_2^T R_{bdn}\bar{\eta}_2 + \bar{\eta}_3^T R_{bdn}\bar{\eta}_3,$$
$$\Xi = \begin{bmatrix} \Xi_{11} & * & * & * \\ \Xi_{21} & \Xi_{22} & * & * \\ \Xi_{31} & 0 & \Xi_{33} & * \\ \Xi_{41} & 0 & 0 & \Xi_{44} \end{bmatrix},$$
$$\bar{\eta}_1 = \begin{bmatrix} \eta_1\ 0\ 0\ 0 \end{bmatrix}, \quad \bar{\eta}_2 = \begin{bmatrix} \eta_2\ 0\ 0\ 0 \end{bmatrix}, \quad \bar{\eta}_3 = \begin{bmatrix} \eta_3\ 0\ 0\ 0 \end{bmatrix},$$
$$\eta_1 = \begin{bmatrix} \tilde{A}\ \bar{\alpha} I_1 L\tilde{C}\ \tilde{B}KI_2\ \bar{\beta}\hat{B}KI_3\ 0\ 0\ 0 \end{bmatrix},$$
$$\eta_2 = \begin{bmatrix} 0\ \alpha_1 I_1 L\tilde{C}\ 0\ 0\ 0\ 0\ 0 \end{bmatrix},$$
$$\eta_3 = \begin{bmatrix} 0\ 0\ 0\ \beta_1\hat{B}KI_3\ 0\ 0\ 0 \end{bmatrix},$$
$$\mu = \sum_{b\in\Omega_k^a}\mu_{ab}, \quad \bar{\mu} = \sum_{b\in\Omega_{uk}^a}\mu_{ab}, \quad \nu = \sum_{d\in\Lambda_k^c}\nu_{cd},$$
$$\bar{\nu} = \sum_{d\in\Lambda_{uk}^c}\nu_{cd}, \sigma = \sum_{n\in\Upsilon_k^m}\sigma_{mn}, \bar{\sigma} = \sum_{n\in\Upsilon_{uk}^m}\sigma_{mn}.$$

Let $S_{bdn} = R_{bdn}^{-1}$, and one can get (40) by using the Schur Complement again.

$$\mu\nu\sigma\left(\Xi + \bar{\eta}_1^T R_{bdn}\bar{\eta}_1 + \bar{\eta}_2^T R_{bdn}\bar{\eta}_2 + \bar{\eta}_3^T R_{bdn}\bar{\eta}_3\right) = \begin{bmatrix} \mu\nu\sigma\,\Xi & * \\ \tilde{\mathrm{X}}_{\Omega_k^a\Lambda_k^c\Upsilon_k^m} & \Psi_{\Omega_k^a\Lambda_k^c\Upsilon_k^m} \end{bmatrix} < 0 \tag{40}$$

where

$$\Psi_{\Omega_k^a\Lambda_k^c\Upsilon_k^m} = diag\left\{\tilde{\Psi}_{\Omega_k^a\Lambda_k^c\Upsilon_k^m}\ \tilde{\Psi}_{\Omega_k^a\Lambda_k^c\Upsilon_k^m}\ \tilde{\Psi}_{\Omega_k^a\Lambda_k^c\Upsilon_k^m}\right\},$$
$$\tilde{\Psi}_{\Omega_k^a\Lambda_k^c\Upsilon_k^m} = diag\{-S_{\Omega_1^a\Lambda_1^c\Upsilon_1^m} \cdots - S_{\Omega_p^a\Lambda_r^c\Upsilon_t^m}\},$$

$$
\begin{aligned}
X^T_{\Omega^a_k\Lambda^c_k\Upsilon^m_k} &= \left[\tilde{X}^T_{1\Omega^a_k\Lambda^c_k\Upsilon^m_k}\ \tilde{X}^T_{2\Omega^a_k\Lambda^c_k\Upsilon^m_k}\ \tilde{X}^T_{3\Omega^a_k\Lambda^c_k\Upsilon^m_k}\right],\\
\tilde{X}^T_{1\Omega^a_k\Lambda^c_k\Upsilon^m_k} &= [\sqrt{\mu_{a\Omega^a_1}\nu_{c\Lambda^c_1}\sigma_{m\Upsilon^m_1}}\bar{\eta}^T_1\cdots\sqrt{\mu_{a\Omega^a_p}\nu_{c\Lambda^c_r}\sigma_{m\Upsilon^m_t}}\bar{\eta}^T_1],\\
\tilde{X}^T_{2\Omega^a_k\Lambda^c_k\Upsilon^m_k} &= [\sqrt{\mu_{a\Omega^a_1}\nu_{c\Lambda^c_1}\sigma_{m\Upsilon^m_1}}\bar{\eta}^T_2\cdots\sqrt{\mu_{a\Omega^a_p}\nu_{c\Lambda^c_r}\sigma_{m\Upsilon^m_t}}\bar{\eta}^T_2],\\
\tilde{X}^T_{3\Omega^a_k\Lambda^c_k\Upsilon^m_k} &= [\sqrt{\mu_{a\Omega^a_1}\nu_{c\Lambda^c_1}\sigma_{m\Upsilon^m_1}}\bar{\eta}^T_3\cdots\sqrt{\mu_{a\Omega^a_p}\nu_{c\Lambda^c_r}\sigma_{m\Upsilon^m_t}}\bar{\eta}^T_3].
\end{aligned}
$$

By substituting $\tilde{A} = \tilde{A}_0 + \tilde{D}_1\tilde{F}_1\tilde{E}_1$, $\tilde{B} = \tilde{B}_0 + \tilde{D}_2\tilde{F}_2\tilde{E}_2, \hat{B} = \hat{B}_0 + \tilde{D}_3\tilde{F}_3\tilde{E}_3$ into (40), it can be decomposed into the certain part and the uncertain part. According Lemma 2, we have

$$
\begin{aligned}
&\begin{bmatrix}\mu\nu\sigma\,\Xi & *\\ \tilde{X}_{\Omega^a_k\Lambda^c_k\Upsilon^m_k}\Psi_{\Omega^a_k\Lambda^c_k\Upsilon^m_k} & \end{bmatrix} = \begin{bmatrix}\mu\nu\sigma\,\tilde{\Xi}_0 & *\\ X_{\Omega^a_k\Lambda^c_k\Upsilon^m_k}\Psi_{\Omega^a_k\Lambda^c_k\Upsilon^m_k} & \end{bmatrix}\\
&\quad + D_{\Omega^a_k\Lambda^c_k\Upsilon^m_k}FE_{\Omega^a_k\Lambda^c_k\Upsilon^m_k} + E^T_{\Omega^a_k\Lambda^c_k\Upsilon^m_k}F^TD^T_{\Omega^a_k\Lambda^c_k\Upsilon^m_k}\\
&\quad \le \begin{bmatrix}\mu\nu\sigma\,\tilde{\Xi}_0 & *\\ X_{\Omega^a_k\Lambda^c_k\Upsilon^m_k}\Psi_{\Omega^a_k\Lambda^c_k\Upsilon^m_k} & \end{bmatrix} + \varepsilon_1 D_{\Omega^a_k\Lambda^c_k\Upsilon^m_k}D^T_{\Omega^a_k\Lambda^c_k\Upsilon^m_k}\\
&\quad + \varepsilon_1^{-1}EN^T_{\Omega^a_k\Lambda^c_k\Upsilon^m_k}E_{\Omega^a_k\Lambda^c_k\Upsilon^m_k}
\end{aligned}
\tag{41}
$$

or equivalently

$$
\begin{bmatrix}
\mu\nu\sigma\,\tilde{\Xi}_0 & * & * & * & * & *\\
X_{\Omega^a_k\Lambda^c_k\Upsilon^m_k} & \Psi_{\Omega^a_k\Lambda^c_k\Upsilon^m_k} & * & * & * & *\\
\varepsilon_1\tilde{D}^T & 0 & -\varepsilon_1 I & * & * & *\\
0 & \varepsilon_1\tilde{D}^T_{\Omega^a_k\Lambda^c_k\Upsilon^m_k} & 0 & -\varepsilon_1 I & * & *\\
\tilde{E} & 0 & 0 & 0 & -\varepsilon_1 I & *\\
\tilde{E}_{\Omega^a_k\Lambda^c_k\Upsilon^m_k} & 0 & 0 & 0 & 0 & -\varepsilon_1 I
\end{bmatrix} < 0 \tag{42}
$$

where the definition of parameters in (41) is given in Appendix B.

The matrix inequality in (42) still contains Q_1, Q_1^{-1}, Q_2, Q_2^{-1}, Q_3, Q_3^{-1}. To convert (42) into LMI (30), the inequality $-Q_1^{-1} < -2I + Q_1$ is used since $\left(I - X_1^{-1}\right)\left(I - X_1^{-1}\right) > 0 \Leftrightarrow -X_1^{-1} < -2I + X_1$ [55], so we can get (43).

$$
\begin{aligned}
\Xi_0 &= \begin{bmatrix}\Xi_{11} & * & * & *\\ \Xi_{210} & \tilde{\Xi}_{22} & * & *\\ \Xi_{310} & 0 & \tilde{\Xi}_{33} & *\\ \Xi_{410} & 0 & 0 & \tilde{\Xi}_{44}\end{bmatrix},\\
\tilde{\Xi}_{22} &= diag\left\{-2I + Q_1\ -2I + Q_1\ -2I + Q_1\right\},\\
\tilde{\Xi}_{33} &= diag\left\{-2I + Q_2\ -2I + Q_2\ -2I + Q_2\right\},\\
\tilde{\Xi}_{44} &= diag\left\{-2I + Q_3\ -2I + Q_3\ -2I + Q_3\right\}.
\end{aligned}
\tag{43}
$$

Since $\mu_{ab} > 0, \nu_{cd} > 0, \sigma_{mn} > 0$, if (30) - (37) hold, then (19) holds, that is, the closed-loop system (13) is stochastically stable. This ends the proof.

V. SIMULATION ANALYSIS

In this section, the effectiveness and generalization performance of the cloud controller designed in this paper are verified through simulation experiments of typical plants.

A. EFFECTIVENESS OF THE CLOUD CONTROLLER

Example 1: Consider the interval controlled plant with the following parameters:

$$
A_1 = \begin{bmatrix}[0.42, 0.62] & [-0.79, -0.59]\\ [-0.1, 0.1] & [0.09, 0.29]\end{bmatrix},\ B_1 = \begin{bmatrix}[0.2, 0.4]\\ [0.1, 0.3]\end{bmatrix},\ C = \begin{bmatrix}1.5 & 0.7\\ 0.2 & 0.4\end{bmatrix},
$$

where the coefficients of the nominal system are

$$
A_0 = \begin{bmatrix}0.52 & -0.69\\ 0 & 0.19\end{bmatrix},\quad B_0 = \begin{bmatrix}0.3\\ 0.2\end{bmatrix},\quad C = \begin{bmatrix}1.5 & 0.7\\ 0.2 & 0.4\end{bmatrix}.
$$

Assume feedback channel time-delay $\tau_k^{sc} \in \Omega = \{0, 1\}$, forward channel time-delay $\tau_k^{ca} \in \tilde{\Upsilon} = \{0, 1\}$ and cloud controller time-delay $\tau_k^c \in \Lambda = \{0, 1\}$, and the transition probability matrices of which are as follows:

$$
\Pi_{sc} = \begin{bmatrix}0.8 & 0.2\\ ? & ?\end{bmatrix},\quad \Pi_{ca} = \begin{bmatrix}? & ?\\ 0.7 & 0.3\end{bmatrix},\quad \Pi_c = \begin{bmatrix}0.8 & 0.2\\ ? & ?\end{bmatrix}.
$$

The sum of forward channel time-delay and cloud controller time-delay is $\psi_k \in \Upsilon = \{0, 1, 2\}$, and the transition probability matrix of which is

$$
\Pi_{ca+c} = \begin{bmatrix}? & ? & ?\\ 0.56 & 0.38 & 0.06\\ ? & ? & ?\end{bmatrix}.
$$

The packet loss probability is $1 - E\{\alpha_k\} = 1 - \bar{\alpha} = 1 - E\{\beta_k\} = 1 - \bar{\beta} = 0.2$. Assuming that the observer parameters are uncertain, take them as the interval values whose midpoint values are the same as the ones of the corresponding coefficients of the controlled plant, but the widths are different, that is,

$$
A_2 = \begin{bmatrix}[0.47, 0.57] & [-0.74, -0.64]\\ [-0.05, 0.05] & [0.14, 0.24]\end{bmatrix},\ B_2 = \begin{bmatrix}[0.25, 0.35]\\ [0.15, 0.25]\end{bmatrix}.
$$

By using the MATLAB LMI toolbox, the control law gain matrix and observer gain matrix of the cloud controller considering the uncertainties existing in the cloud, network, and controlled plant can be obtained as

$$
K = \begin{bmatrix}0.0017 & 0.0042\end{bmatrix},\quad L = \begin{bmatrix}0.0068 & 0.0012\\ -0.0082 & 0.0362\end{bmatrix}.
$$

The initial state of the system is $x_0^T = \begin{bmatrix}1 & -0.5\end{bmatrix}^T$. The distributions of τ_k^{sc}, τ_k^c, τ_k^{ca} are shown in Figs. 4-6, respectively. The distributions of α_k, and β_k are shown in Fig. 7 and Fig. 8, respectively. The state response curves under the control of the designed cloud controller in this paper are shown in Fig. 9.

It can be seen that the state response curves of CCS using the proposed cloud controller converge. This means that the cloud controller can effectively compensate for the impact of various uncertainties and keep the system stable, which demonstrates the effectiveness of the proposed cloud controller.

Example 2: Consider the interval controlled plant with the following parameters:

$$
A_1 = \begin{bmatrix}[-0.74, -0.66] & [-0.13, -0.07]\\ [0.95, 1.05] & [0.19, 0.21]\end{bmatrix},
$$

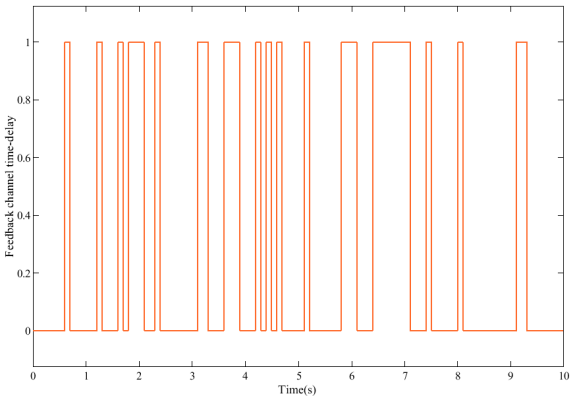

FIGURE 4. Distribution of τ_k^{sc}.

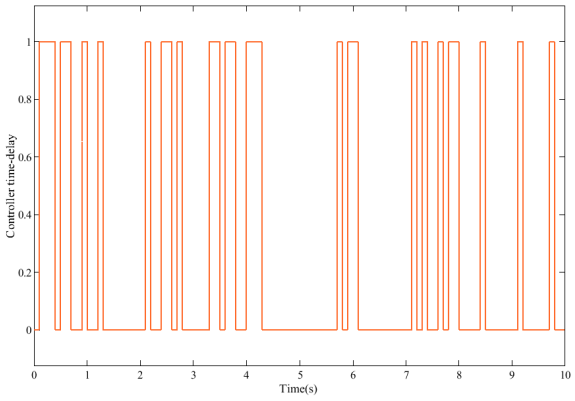

FIGURE 5. Distribution of τ_k^{c}.

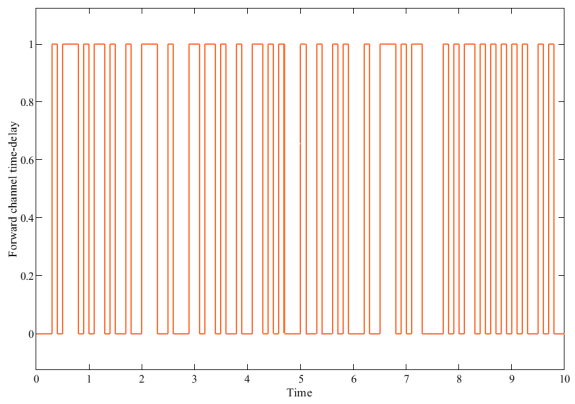

FIGURE 6. Distribution of τ_k^{ca}.

$$B_1 = \begin{bmatrix} [1.8, 2.2] \\ [0.49, 0.51] \end{bmatrix},$$
$$C = \begin{bmatrix} 1 & 0 \end{bmatrix},$$

Obviously, the nominal system is unstable. Assume feedback channel time-delay $\tau_k^{sc} \in \Omega = \{0, 1\}$, forward channel time-delay $\tau_k^{ca} \in \tilde{\Upsilon} = \{0, 1\}$ and cloud controller time-delay $\tau_k^{c} \in \Lambda = \{0, 1\}$, and the transition probability matrices of which are as follows:

$$\Pi_{sc} = \begin{bmatrix} 0.7 & 0.3 \\ ? & ? \end{bmatrix}, \quad \Pi_{ca} = \begin{bmatrix} ? & ? \\ 0.9 & 0.1 \end{bmatrix}, \quad \Pi_{c} = \begin{bmatrix} 0.7 & 0.3 \\ ? & ? \end{bmatrix}.$$

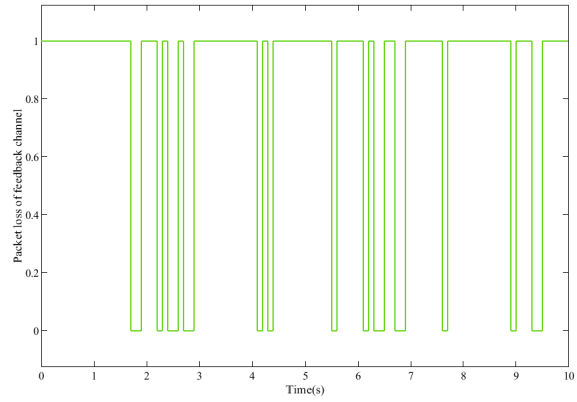

FIGURE 7. Distribution of α_k.

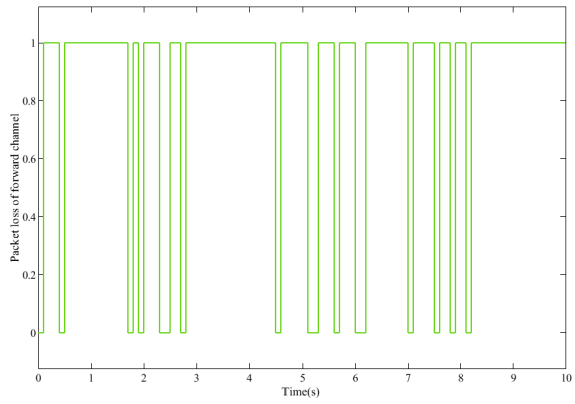

FIGURE 8. Distribution of β_k.

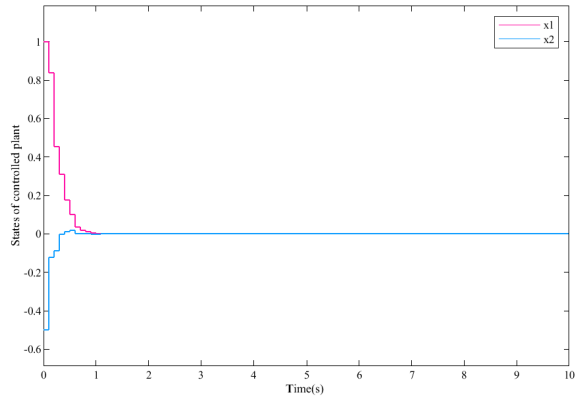

FIGURE 9. State response of the CCS using the proposed cloud controller.

The sum of forward channel time-delay and cloud controller time-delay is $\psi_k \in \Upsilon = \{0, 1, 2\}$, and the transition probability matrix of which is

$$\Pi_{ca+c} = \begin{bmatrix} ? & ? & ? \\ 0.63 & 0.34 & 0.03 \\ ? & ? & ? \end{bmatrix}.$$

The packet loss probability is $1 - E\{\alpha_k\} = 1 - \bar{\alpha} = 1 - E\{\beta_k\} = 1 - \bar{\beta} = 0.2$. Assuming that the observer parameters are uncertain, take them as the interval values, that

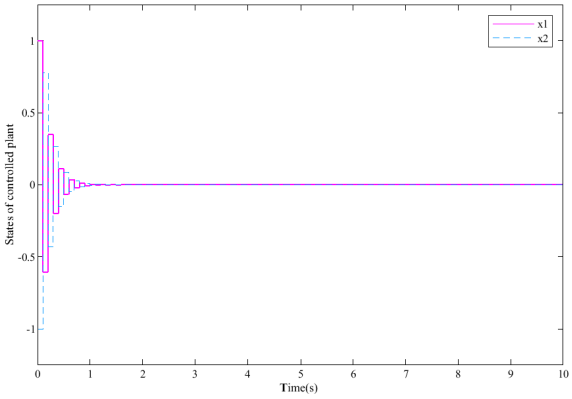

FIGURE 10. State response of the CCS using the proposed cloud controller.

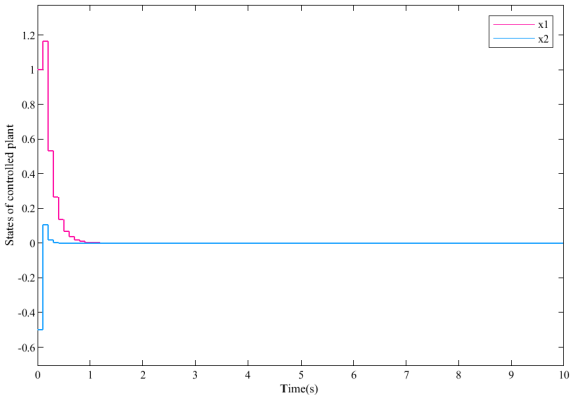

FIGURE 11. State response of the NCS using the proposed cloud controller.

is,

$$A_2 = \begin{bmatrix} [-0.75, -0.65] & [-0.15, -0.05] \\ [0.95, 1.05] & [0.15, 0.25] \end{bmatrix},$$
$$B_2 = \begin{bmatrix} [1.95, 2.05] \\ [0.45, 0.55] \end{bmatrix}.$$

According to Theorem 2, the control law gain matrix and observer gain matrix considering the uncertainties existing in the cloud, network, and controlled plant can be obtained as

$$K = \begin{bmatrix} 0.0010 & 0.0001 \end{bmatrix}, \quad L = \begin{bmatrix} 0.0283 \\ -0.0271 \end{bmatrix}.$$

The initial state of the system is $x_0^T = \begin{bmatrix} 1 & -1 \end{bmatrix}^T$. The state response curves under the control of the designed cloud controller in this paper are shown in Fig. 10.

It can be seen that the state response curves of CCS using the proposed cloud controller converge. The cloud controller can keep the system stable, which demonstrates the effectiveness of the proposed cloud controller.

B. GENERALIZATION PERFORMANCE OF THE CLOUD CONTROLLER

The design of the cloud controller considers the uncertainty existing in the controlled plant, network channel, and controller, so it is not only applicable to the CCS but also applicable to conventional control systems with uncertain controlled plants and the NCS with uncertain controlled plants or network time-delay and packet loss.

For example, when the cloud controller is applied to the NCS with bilateral time-delay and packet loss of network channel, the system state curves can be obtained, as shown in Fig. 11. It can be seen that the system state curves converge and the system keeps stable, which shows the generalization performance of the cloud controller.

VI. CONCLUSION

This paper proposes a new structure framework of the CCS. The system uncertainty is decomposed reasonably, through in-depth analysis of the internal characteristics of the CCS. System modeling is carried out from the control point of view, and the cloud controller is designed by utilizing the Lyapunov stability theorem and LMI method to compensate for or eliminate the impact of all the uncertainties existing in the cloud computing, the network, and the controlled plant. Simulation experiments demonstrate the effectiveness and generalization performance of the cloud controller.

The approach of CCS modeling and controller design proposed in this paper is actually a generalized control system design method. Considering that the deterministic system is a special case of uncertain systems, the proposed structure can also be called a general framework of control system design, which is suitable for designing the controller of a general system based on the stability principle.

In fact, the theory and application research of the CCS is still in a preliminary stage and is facing many difficulties and challenges. The complex characteristics of the cloud, network, and controlled plant need to be further considered. For example, the security of the cloud, the different stochastic characteristics of network and cloud and the coupling between them, and the nonlinear characteristics of the controlled plants need to be studied in the future. In addition, although the cloud controller can be successfully applied to the slow time-varying control system [56], it is also one of the future research directions to apply the cloud controller to the fast time-varying system in the actual environment.

APPENDIX A
PROOF OF THE THEOREM 1

Let $\zeta_k = \xi_{k+1} - \xi_k$, and for the closed-loop system (13), we choose the Lyapnov-Krasovskii function as

$$V_k = \sum_{l=1}^{4} V_l\left(\xi_k, \phi_k, \varphi_k, \psi_k\right) \triangleq \xi_k^T \Phi_{\phi_k,\varphi_k,\psi_k} \xi_k \tag{20}$$

where

$$V_1\left(\xi_k, \phi_k, \varphi_k, \psi_k\right) = \xi_k^T R_{\phi_k,\varphi_k,\psi_k} \xi_k$$
$$V_2\left(\xi_k, \phi_k, \varphi_k, \psi_k\right) = \sum_{\rho=k-\phi_M}^{k-1} \xi_\rho^T P_1 \xi_\rho + \sum_{\rho=k-\varphi_M}^{k-1} \xi_\rho^T P_2 \xi_\rho + \sum_{\rho=k-\psi_M}^{k-1} \xi_\rho^T P_3 \xi_\rho$$

$$
\begin{aligned}
V_3(\xi_k,\phi_k,\varphi_k,\psi_k) = & \sum_{j=-\phi_M+1}^{0}\sum_{i=k+j-1}^{k-1}\xi_i^T P_4\xi_i \\
& + \sum_{\rho=k-\phi_k}^{k-1}\xi_\rho^T P_4\xi_\rho + \sum_{j=-\varphi_M+1}^{0}\sum_{i=k+j-1}^{k-1} \\
& \times \xi_i^T P_5\xi_i + \sum_{\rho=k-\varphi_k}^{k-1}\xi_\rho^T P_5\xi_\rho \\
& + \sum_{j=-\psi_M+1}^{0}\sum_{i=k+j-1}^{k-1}\xi_i^T P_6\xi_i \\
& \sum_{\rho=k-\psi_k}^{k-1}\xi_\rho^T P_6\xi_\rho \\
V_4(\xi_k,\phi_k,\varphi_k,\psi_k) = & \sum_{j=-\phi_M+1}^{0}\sum_{i=k+j-1}^{k-1}\phi_M\zeta_i^T Q_1\zeta_i \\
& + \sum_{j=-\varphi_M+1}^{0}\sum_{i=k+j-1}^{k-1}\varphi_M\zeta_i^T Q_2\zeta_i \\
& + \sum_{j=-\psi_M+1}^{0}\sum_{i=k+j-1}^{k-1}\psi_M\zeta_i^T Q_3\zeta_i.
\end{aligned}
$$

Obviously, we have $\Phi_{\phi_k,\varphi_k,\psi_k} > 0$. By using the Bernoulli distribution properties stated in (1), one can get (21).

$$
\begin{aligned}
& E\{\Delta V_1(\xi_k,\phi_k,\varphi_k,\psi_k)\} \\
& = E\{\xi_{k+1}^T R_{\phi_{k+1},\varphi_{k+1},\psi_{k+1}}\xi_{k+1}\,|_{\phi_k=a,\varphi_k=c,\psi_k=m}\} \\
& \quad - \xi_k^T R_{\phi_k,\varphi_k,\psi_k}\xi_k \\
& = E\{(\tilde{A}\xi_k + (\alpha_k-\bar{\alpha})I_1L\tilde{C}\xi_{k-\phi_k} + \bar{\alpha}I_1L\tilde{C}\xi_{k-\phi_k} \\
& \quad + \tilde{B}KI_2\xi_{k-\varphi_k} + (\beta_k-\bar{\beta})\hat{B}KI_3\xi_{k-\psi_k} \\
& \quad + \bar{\beta}\hat{B}KI_3\xi_{k-\psi_k})^T \sum_{b=0}^{\phi_M}\sum_{d=0}^{\varphi_M}\sum_{n=0}^{\psi_M}\mu_{ab}\nu_{cd}\sigma_{mn}R_{bdn}(\tilde{A}\xi_k \\
& \quad + (\alpha_k-\bar{\alpha})I_1L\tilde{C}\xi_{k-\phi_k} + \bar{\alpha}I_1L\tilde{C}\xi_{k-\phi_k} + \tilde{B}KI_2\xi_{k-\varphi_k} \\
& \quad + (\beta_k-\bar{\beta})\hat{B}KI_3\xi_{k-\psi_k} + \bar{\beta}\hat{B}KI_3\xi_{k-\psi_k})\} - \xi_k^T R_{acm}\xi_k \\
& = \xi_k^T\tilde{A}^T\bar{R}_{bdn}\tilde{A}\xi_k + \xi_k^T\tilde{A}^T\bar{R}_{bdn}\bar{\alpha}I_1L\tilde{C}\xi_{k-\phi_k} \\
& \quad + \xi_k^T\tilde{A}^T\bar{R}_{bdn}\tilde{B}KI_2\xi_{k-\varphi_k} + \xi_k^T\tilde{A}^T\bar{R}_{bdn}\bar{\beta}\hat{B}KI_3\xi_{k-\psi_k} \\
& \quad + \alpha_1^2\xi_{k-\phi_k}^T(I_1L\tilde{C})^T\bar{R}_{bdn}I_1L\tilde{C}\xi_{k-\phi_k} \\
& \quad + \xi_{k-\phi_k}^T(\bar{\alpha}I_1L\tilde{C})^T\bar{R}_{bdn}\tilde{A}\xi_k \\
& \quad + \xi_{k-\phi_k}^T(\bar{\alpha}I_1L\tilde{C})^T\bar{R}_{bdn}\bar{\alpha}I_1L\tilde{C}\xi_{k-\phi_k} \\
& \quad + \xi_{k-\phi_k}^T(\bar{\alpha}I_1L\tilde{C})^T\bar{R}_{bdn}\tilde{B}KI_2\xi_{k-\varphi_k} \\
& \quad + \xi_{k-\phi_k}^T(\bar{\alpha}I_1L\tilde{C})^T\bar{R}_{bdn}\bar{\beta}\hat{B}KI_3\xi_{k-\psi_k} \\
& \quad + \xi_{k-\varphi_k}^T(\tilde{B}KI_2)^T\bar{R}_{bdn}\tilde{A}\xi_k \\
& \quad + \xi_{k-\varphi_k}^T(\tilde{B}KI_2)^T\bar{R}_{bdn}\bar{\alpha}I_1L\tilde{C}\xi_{k-\phi_k} \\
& \quad + \xi_{k-\varphi_k}^T(\tilde{B}KI_2)^T\bar{R}_{bdn}\tilde{B}KI_2\xi_{k-\varphi_k} \\
& \quad + \xi_{k-\varphi_k}^T(\tilde{B}KI_2)^T\bar{R}_{bdn}\bar{\beta}\hat{B}KI_3\xi_{k-\psi_k} \\
& \quad + \beta_1^2\xi_{k-\psi_k}^T(\hat{B}KI_3)^T\bar{R}_{bdn}\hat{B}KI_3\xi_{k-\psi_k} \\
& \quad + \xi_{k-\psi_k}^T(\bar{\beta}\hat{B}KI_3)^T\bar{R}_{bdn}\tilde{A}\xi_k \\
& \quad + \xi_{k-\psi_k}^T(\bar{\beta}\hat{B}KI_3)^T\bar{R}_{bdn}\bar{\alpha}I_1L\tilde{C}\xi_{k-\phi_k} \\
& \quad + \xi_{k-\psi_k}^T(\bar{\beta}\hat{B}KI_3)^T\bar{R}_{bdn}\tilde{B}KI_2\xi_{k-\varphi_k} \\
& \quad + \xi_{k-\psi_k}^T(\bar{\beta}\hat{B}KI_3)^T\bar{R}_{bdn}\bar{\beta}\hat{B}KI_3\xi_{k-\psi_k} - \xi_k^T R_{acm}\xi_k \qquad (21)
\end{aligned}
$$

$$
\begin{aligned}
& E\{\Delta V_2(\xi_k,\phi_k,\varphi_k,\psi_k)\} = \xi_k^T P_1\xi_k - \xi_{k-\phi_M}^T P_1\xi_{k-\phi_M} \\
& \quad + \xi_k^T P_2\xi_k - \xi_{k-\varphi_M}^T P_2\xi_{k-\varphi_M} + \xi_k^T P_3\xi_k - \xi_{k-\psi_M}^T P_3\xi_{k-\psi_M} \qquad (22)
\end{aligned}
$$

$$
\begin{aligned}
& E\{\Delta V_3(\xi_k,\phi_k,\varphi_k,\psi_k)\} \\
& = \phi_M\xi_k^T P_4\xi_k - \sum_{\rho=k-\phi_M}^{k-1}\xi_\rho^T P_4\xi_\rho + \sum_{\rho=k+1-\phi_{k+1}}^{k}\xi_\rho^T P_4\xi_\rho \\
& \quad - \sum_{\rho=k-\phi_k}^{k-1}\xi_\rho^T P_4\xi_\rho + \varphi_M\xi_k^T P_5\xi_k - \sum_{\rho=k-\varphi_M}^{k-1}\xi_\rho^T P_5\xi_\rho \\
& \quad + \sum_{\rho=k+1-\varphi_{k+1}}^{k}\xi_\rho^T P_5\xi_\rho - \sum_{\rho=k-\varphi_k}^{k-1}\xi_\rho^T P_5\xi_\rho + \psi_M\xi_k^T P_6\xi_k \\
& \quad - \sum_{\rho=k-\psi_M}^{k-1}\xi_\rho^T P_6\xi_\rho + \sum_{\rho=k+1-\psi_{k+1}}^{k}\xi_\rho^T P_6\xi_\rho - \sum_{\rho=k-\psi_k}^{k-1}\xi_\rho^T P_6\xi_\rho
\end{aligned} \qquad (23)
$$

Since

$$
\begin{aligned}
& - \sum_{\rho=k-\phi_M}^{k-1}\xi_\rho^T P_4\xi_\rho + \sum_{\rho=k+1-\phi_{k+1}}^{k}\xi_\rho^T P_4\xi_\rho - \sum_{\rho=k-\phi_k}^{k-1}\xi_\rho^T P_4\xi_\rho \\
& = - \sum_{\rho=k-\phi_M}^{k-1}\xi_\rho^T P_4\xi_\rho + \xi_k^T P_4\xi_k - \xi_{k-\phi_k}^T P_4\xi_{k-\phi_k} \\
& \quad + \sum_{\rho=k+1-\phi_{k+1}}^{k-\phi_k}\xi_\rho^T P_4\xi_\rho + \sum_{\rho=k+1-\phi_k}^{k-1}\xi_\rho^T P_4\xi_\rho - \sum_{\rho=k+1-\phi_k}^{k-1}\xi_\rho^T P_4\xi_\rho \\
& \le 2\xi_k^T P_4\xi_k - \xi_{k-\phi_k}^T P_4\xi_{k-\phi_k},
\end{aligned}
$$

one can obtain

$$
\begin{aligned}
& E\{\Delta V_3(\xi_k,\phi_k,\varphi_k,\psi_k)\} \le (\phi_M+2)\xi_k^T P_4\xi_k \\
& \quad - \xi_{k-\phi_k}^T P_4\xi_{k-\phi_k} + (\varphi_M+2)\xi_k^T P_5\xi_k - \xi_{k-\varphi_k}^T P_5\xi_{k-\varphi_k} \\
& \quad + (\psi_M+2)\xi_k^T P_6\xi_k - \xi_{k-\psi_k}^T P_6\xi_{k-\psi_k} \qquad (24)
\end{aligned}
$$

$$
\begin{aligned}
& E\{\Delta V_4(\xi_k,\phi_k,\varphi_k,\psi_k)\} \\
& = E\{\phi_M^2\zeta_k^T Q_1\zeta_k\} - \sum_{\rho=k-\phi_M}^{k-1}\phi_M\zeta_\rho^T Q_1\zeta_\rho + E\{\varphi_M^2\zeta_k^T Q_2\zeta_k\} \\
& \quad - \sum_{\rho=k-\varphi_M}^{k-1}\varphi_M\zeta_\rho^T Q_2\zeta_\rho + E\{\psi_M^2\zeta_k^T Q_3\zeta_k\} - \sum_{\rho=k-\psi_M}^{k-1}\psi_M\zeta_\rho^T Q_3\zeta_\rho
\end{aligned} \qquad (25)
$$

Note that

$$
\begin{aligned}
& E\{\phi_M^2\zeta_k^T Q_1\zeta_k\} = \phi_M^2 E\{((\tilde{A}-I)\xi_k + (\alpha_k-\bar{\alpha})I_1L\tilde{C}\xi_{k-\phi_k} \\
& \quad + \bar{\alpha}I_1L\tilde{C}\xi_{k-\phi_k} + \tilde{B}KI_2\xi_{k-\varphi_k} + (\beta_k-\bar{\beta})\hat{B}KI_3\xi_{k-\psi_k} \\
& \quad + \bar{\beta}\hat{B}KI_3\xi_{k-\psi_k})^T Q_1((\tilde{A}-I)\xi_k + (\alpha_k-\bar{\alpha})I_1L\tilde{C}\xi_{k-\phi_k} \\
& \quad + \bar{\alpha}I_1L\tilde{C}\xi_{k-\phi_k} + \tilde{B}KI_2\xi_{k-\varphi_k} + (\beta_k-\bar{\beta})\hat{B}KI_3\xi_{k-\psi_k} \\
& \quad + \bar{\beta}\hat{B}KI_3\xi_{k-\psi_k})\}
\end{aligned} \qquad (26)
$$

By Lemma 1, one can obtain

$$
\begin{aligned}
&-\sum_{\rho=k-\phi_M}^{k-1}\phi_M\zeta_\rho^T Q_1\zeta_\rho \\
&\le -\sum_{\rho=k-\phi_k}^{k-1}\phi_k\zeta_\rho^T Q_1\zeta_\rho-\sum_{\rho=k-\phi_M}^{k-\phi_k-1}(\phi_M-\phi_k)\,\zeta_\rho^T Q_1\zeta_\rho \\
&\le -\left[\xi_k-\xi_{k-\phi_k}\right]^T Q_1\left[\xi_k-\xi_{k-\phi_k}\right] \\
&\quad -\left[\xi_{k-\phi_k}-\xi_{k-\phi_M}\right]^T Q_1\left[\xi_{k-\phi_k}-\xi_{k-\phi_M}\right] \qquad (27)
\end{aligned}
$$

From (21) - (27), one can get

$$
E\{\Delta V_k\}\le\chi_k^T\Gamma\chi_k\le-\lambda_{\min}(-\Gamma)\chi_k^T\chi_k\le-\varepsilon\|\chi_k\|^2\le-\varepsilon\|\xi_k\|^2 \qquad (28)
$$

where,

$$
\begin{aligned}
\chi_k &= \left[\xi_k^T\ \xi_{k-\phi_k}^T\ \xi_{k-\varphi_k}^T\ \xi_{k-\psi_k}^T\ \xi_{k-\phi_M}^T\ \xi_{k-\varphi_M}^T\ \xi_{k-\psi_M}^T\right]^T, \\
\varepsilon &= \inf\{-\lambda_{\min}(-\Gamma)\}>0.
\end{aligned}
$$

From (28), one can obtain (29) for any positive integer $T\ge 1$.

$$
\begin{aligned}
E\left\{\sum_{k=0}^{\infty}\|\xi_k\|^2\right\} &\le 1/\varepsilon E\{V_0\}-1/\varepsilon E\{V_{T+1}\} \\
&\le 1/\varepsilon E\{V_0\}=1/\varepsilon\xi_0^T\Phi_{\phi_0,\varphi_0,\psi_0}\xi_k \qquad (29)
\end{aligned}
$$

According to Definition 1, the closed-loop CCS is stochastically stable, and the proof is completed.

APPENDIX B
DEFINITION OF PARAMETERS
A. DEFINITION OF PARAMETERS IN (30)-(37)

$$
\begin{aligned}
\Psi_{\Omega_k^a\Lambda_k^c\Upsilon_k^m} &= diag\left\{\tilde\Psi_{\Omega_k^a\Lambda_k^c\Upsilon_k^m}\ \tilde\Psi_{\Omega_k^a\Lambda_k^c\Upsilon_k^m}\ \tilde\Psi_{\Omega_k^a\Lambda_k^c\Upsilon_k^m}\right\},\\
\tilde\Psi_{\Omega_k^a\Lambda_k^c\Upsilon_k^m} &= diag\{-S_{\Omega_1^a\Lambda_1^c\Upsilon_1^m}\cdots-S_{\Omega_p^a\Lambda_r^c\Upsilon_t^m}\},\\
X^T_{\Omega_k^a\Lambda_k^c\Upsilon_k^m} &= \left[\check X^T_{1\Omega_k^a\Lambda_k^c\Upsilon_k^m}\ \check X^T_{2\Omega_k^a\Lambda_k^c\Upsilon_k^m}\ \check X^T_{3\Omega_k^a\Lambda_k^c\Upsilon_k^m}\right],\\
\check X^T_{i\Omega_k^a\Lambda_k^c\Upsilon_k^m} &= [\sqrt{\mu_a\Omega_1^a\nu_{c\Lambda_1^c}\sigma_m\Upsilon_1^m}\tilde\eta_i^T\cdots\sqrt{\mu_a\Omega_p^a\nu_{c\Lambda_r^c}\sigma_m\Upsilon_t^m}\tilde\eta_i^T],\\
\tilde D_{\Omega_k^a\Lambda_k^c\Upsilon_k^m} &= diag\left\{\tilde D_{1\Omega_k^a\Lambda_k^c\Upsilon_k^m}\ \tilde D_{2\Omega_k^a\Lambda_k^c\Upsilon_k^m}\ \tilde D_{3\Omega_k^a\Lambda_k^c\Upsilon_k^m}\right\},\\
\tilde D_{i\Omega_k^a\Lambda_k^c\Upsilon_k^m} &= diag\{\sqrt{\mu_a\Omega_1^a\nu_{c\Lambda_1^c}\sigma_m\Upsilon_1^m}\bar D_i\cdots\sqrt{\mu_a\Omega_p^a\nu_{c\Lambda_r^c}\sigma_m\Upsilon_t^m}\bar D_i\},\\
\tilde E^T_{\Omega_k^a\Lambda_k^c\Upsilon_k^m} &= \left[\bar E^T_{\Omega_k^a\Lambda_k^c\Upsilon_k^m}\ \bar E^T_{\Omega_k^a\Lambda_k^c\Upsilon_k^m}\ \bar E^T_{\Omega_k^a\Lambda_k^c\Upsilon_k^m}\right],\\
\bar E^T_{\Omega_k^a\Lambda_k^c\Upsilon_k^m} &= [\sqrt{\mu_a\Omega_1^a\nu_{c\Lambda_1^c}\sigma_m\Upsilon_1^m}\hat E^T\cdots\sqrt{\mu_a\Omega_p^a\nu_{c\Lambda_r^c}\sigma_m\Upsilon_t^m}\hat E^T],\\
\Psi_{\Omega_k^a\Lambda_{uk}^c\Upsilon_k^m} &= diag\left\{\tilde\Psi_{\Omega_k^a\Lambda_{uk}^c\Upsilon_k^m}\ \tilde\Psi_{\Omega_k^a\Lambda_{uk}^c\Upsilon_k^m}\ \tilde\Psi_{\Omega_k^a\Lambda_{uk}^c\Upsilon_k^m}\right\},\\
\tilde\Psi_{\Omega_k^a\Lambda_{uk}^c\Upsilon_k^m} &= diag\{-S_{\Omega_1^ad\Upsilon_1^m}\cdots-S_{\Omega_p^ad\Upsilon_t^m}\},\\
X^T_{\Omega_k^a\Lambda_{uk}^c\Upsilon_k^m} &= \left[\check X^T_{1\Omega_k^a\Lambda_{uk}^c\Upsilon_k^m}\ \check X^T_{2\Omega_k^a\Lambda_{uk}^c\Upsilon_k^m}\ \check X^T_{3\Omega_k^a\Lambda_{uk}^c\Upsilon_k^m}\right],\\
\check X^T_{i\Omega_k^a\Lambda_{uk}^c\Upsilon_k^m} &= [\sqrt{\mu_a\Omega_1^a\sigma_m\Upsilon_1^m}\tilde\eta_i^T\cdots\sqrt{\mu_a\Omega_p^a\sigma_m\Upsilon_t^m}\tilde\eta_i^T],\\
\tilde D_{\Omega_k^a\Lambda_{uk}^c\Upsilon_k^m} &= diag\{\tilde D_{1\Omega_k^a\Lambda_{uk}^c\Upsilon_k^m}\tilde D_{2\Omega_k^a\Lambda_{uk}^c\Upsilon_k^m}\tilde D_{3\Omega_k^a\Lambda_{uk}^c\Upsilon_k^m}\},\\
\tilde D_{i\Omega_k^a\Lambda_{uk}^c\Upsilon_k^m} &= diag\{\sqrt{\mu_a\Omega_1^a\sigma_m\Upsilon_1^m}\bar D_i\cdots\sqrt{\mu_a\Omega_p^a\sigma_m\Upsilon_t^m}\bar D_i\},
\end{aligned}
$$

$$
\begin{aligned}
\tilde E^T_{\Omega_k^a\Lambda_{uk}^c\Upsilon_k^m} &= \left[\bar E^T_{\Omega_k^a\Lambda_{uk}^c\Upsilon_k^m}\ \bar E^T_{\Omega_k^a\Lambda_{uk}^c\Upsilon_k^m}\ \bar E^T_{\Omega_k^a\Lambda_{uk}^c\Upsilon_k^m}\right],\\
\bar E^T_{\Omega_k^a\Lambda_{uk}^c\Upsilon_k^m} &= [\sqrt{\mu_a\Omega_1^a\sigma_m\Upsilon_1^m}\hat E^T\cdots\sqrt{\mu_a\Omega_p^a\sigma_m\Upsilon_t^m}\hat E^T],\\
\Psi_{\Omega_{uk}^a\Lambda_k^c\Upsilon_k^m} &= diag\left\{\tilde\Psi_{\Omega_{uk}^a\Lambda_k^c\Upsilon_k^m}\ \tilde\Psi_{\Omega_{uk}^a\Lambda_k^c\Upsilon_k^m}\ \tilde\Psi_{\Omega_{uk}^a\Lambda_k^c\Upsilon_k^m}\right\},\\
\tilde\Psi_{\Omega_{uk}^a\Lambda_k^c\Upsilon_k^m} &= diag\{-S_{b\Lambda_1^c\Upsilon_1^m}\cdots-S_{b\Lambda_r^c\Upsilon_t^m}\},\\
X^T_{\Omega_{uk}^a\Lambda_k^c\Upsilon_k^m} &= \left[\check X^T_{1\Omega_{uk}^a\Lambda_k^c\Upsilon_k^m}\ \check X^T_{2\Omega_{uk}^a\Lambda_k^c\Upsilon_k^m}\ \check X^T_{3\Omega_{uk}^a\Lambda_k^c\Upsilon_k^m}\right],\\
\check X^T_{i\Omega_{uk}^a\Lambda_k^c\Upsilon_k^m} &= [\sqrt{\nu_{c\Lambda_1^c}\sigma_m\Upsilon_1^m}\tilde\eta_i^T\cdots\sqrt{\nu_{c\Lambda_r^c}\sigma_m\Upsilon_t^m}\tilde\eta_i^T],\\
\tilde D_{\Omega_{uk}^a\Lambda_k^c\Upsilon_k^m} &= diag\left\{\tilde D_{1\Omega_{uk}^a\Lambda_k^c\Upsilon_k^m}\tilde D_{2\Omega_{uk}^a\Lambda_k^c\Upsilon_k^m}\tilde D_{3\Omega_{uk}^a\Lambda_k^c\Upsilon_k^m}\right\},\\
\tilde D_{i\Omega_{uk}^a\Lambda_k^c\Upsilon_k^m} &= diag\{\sqrt{\nu_{c\Lambda_1^c}\sigma_m\Upsilon_1^m}\bar D_i\cdots\sqrt{\nu_{c\Lambda_r^c}\sigma_m\Upsilon_t^m}\bar D_i\},\\
\tilde E^T_{\Omega_{uk}^a\Lambda_k^c\Upsilon_k^m} &= \left[\bar E^T_{\Omega_{uk}^a\Lambda_k^c\Upsilon_k^m}\ \bar E^T_{\Omega_{uk}^a\Lambda_k^c\Upsilon_k^m}\ \bar E^T_{\Omega_{uk}^a\Lambda_k^c\Upsilon_k^m}\right],\\
\bar E^T_{\Omega_{uk}^a\Lambda_k^c\Upsilon_k^m} &= [\sqrt{\nu_{c\Lambda_1^c}\sigma_m\Upsilon_1^m}\hat E^T\cdots\sqrt{\nu_{c\Lambda_r^c}\sigma_m\Upsilon_t^m}\hat E^T],\\
\Psi_{\Omega_{uk}^a\Lambda_{uk}^c\Upsilon_k^m} &= diag\left\{\tilde\Psi_{\Omega_{uk}^a\Lambda_{uk}^c\Upsilon_k^m}\ \tilde\Psi_{\Omega_{uk}^a\Lambda_{uk}^c\Upsilon_k^m}\ \tilde\Psi_{\Omega_{uk}^a\Lambda_{uk}^c\Upsilon_k^m}\right\},\\
\tilde\Psi_{\Omega_{uk}^a\Lambda_{uk}^c\Upsilon_k^m} &= diag\{-S_{b\Lambda_1^cn}\cdots-S_{b\Lambda_r^cn}\},\\
X^T_{\Omega_{uk}^a\Lambda_{uk}^c\Upsilon_k^m} &= \left[\check X^T_{1\Omega_{uk}^a\Lambda_{uk}^c\Upsilon_k^m}\ \check X^T_{2\Omega_{uk}^a\Lambda_{uk}^c\Upsilon_k^m}\ \check X^T_{3\Omega_{uk}^a\Lambda_{uk}^c\Upsilon_k^m}\right],\\
\check X^T_{i\Omega_{uk}^a\Lambda_{uk}^c\Upsilon_k^m} &= [\sqrt{\nu_{c\Lambda_1^c}}\tilde\eta_i^T\cdots\sqrt{\nu_{c\Lambda_r^c}}\tilde\eta_i^T],\\
\tilde D_{\Omega_{uk}^a\Lambda_{uk}^c\Upsilon_k^m} &= diag\left\{\tilde D_{1\Omega_{uk}^a\Lambda_{uk}^c\Upsilon_{uk}^m}\tilde D_{2\Omega_{uk}^a\Lambda_{uk}^c\Upsilon_{uk}^m}\tilde D_{3\Omega_{uk}^a\Lambda_{uk}^c\Upsilon_{uk}^m}\right\},\\
\tilde D_{i\Omega_{uk}^a\Lambda_{uk}^c\Upsilon_{uk}^m} &= diag\{\sqrt{\nu_{c\Lambda_1^c}}\bar D_i\cdots\sqrt{\nu_{c\Lambda_r^c}}\bar D_i\},\\
\tilde E^T_{\Omega_{uk}^a\Lambda_{uk}^c\Upsilon_{uk}^m} &= \left[\bar E^T_{\Omega_{uk}^a\Lambda_{uk}^c\Upsilon_{uk}^m}\ \bar E^T_{\Omega_{uk}^a\Lambda_{uk}^c\Upsilon_{uk}^m}\ \bar E^T_{\Omega_{uk}^a\Lambda_{uk}^c\Upsilon_{uk}^m}\right],\\
\bar E^T_{\Omega_{uk}^a\Lambda_{uk}^c\Upsilon_{uk}^m} &= [\sqrt{\nu_{c\Lambda_1^c}}\hat E^T\cdots\sqrt{\nu_{c\Lambda_r^c}}\hat E^T],
\end{aligned}
$$

$$\Psi_{\Omega^a_{uk}\Lambda^c_{uk}\Upsilon^m_k} = diag\left\{\tilde{\Psi}_{\Omega^a_{uk}\Lambda^c_{uk}\Upsilon^m_k}\ \tilde{\Psi}_{\Omega^a_{uk}\Lambda^c_{uk}\Upsilon^m_k}\ \tilde{\Psi}_{\Omega^a_{uk}\Lambda^c_{uk}\Upsilon^m_k}\right\},$$
$$\tilde{\Psi}_{\Omega^a_{uk}\Lambda^c_{uk}\Upsilon^m_k} = diag\{-S_{bd}\Upsilon^m_1 \cdots - S_{bd}\Upsilon^m_t\},$$
$$X^T_{\Omega^a_{uk}\Lambda^c_{uk}\Upsilon^m_k} = \left[\check{X}^T_{1\Omega^a_{uk}\Lambda^c_{uk}\Upsilon^m_k}\ \check{X}^T_{2\Omega^a_{uk}\Lambda^c_{uk}\Upsilon^m_k}\ \check{X}^T_{3\Omega^a_{uk}\Lambda^c_{uk}\Upsilon^m_k}\right],$$
$$\check{X}^T_{i\Omega^a_{uk}\Lambda^c_{uk}\Upsilon^m_k} = [\sqrt{\sigma_m\Upsilon^m_1}\tilde{\eta}^T_i \cdots \sqrt{\sigma_m\Upsilon^m_t}\tilde{\eta}^T_i],$$
$$\tilde{D}_{\Omega^a_{uk}\Lambda^c_{uk}\Upsilon^m_k} = diag\left\{\tilde{D}_{1\Omega^a_{uk}\Lambda^c_{uk}\Upsilon^m_k}\ \tilde{D}_{2\Omega^a_{uk}\Lambda^c_{uk}\Upsilon^m_k}\ \tilde{D}_{3\Omega^a_{uk}\Lambda^c_{uk}\Upsilon^m_k}\right\},$$
$$\tilde{D}_{i\Omega^a_{uk}\Lambda^c_{uk}\Upsilon^m_k} = diag\{\sqrt{\sigma_m\Upsilon^m_1}\bar{D}_i \cdots \sqrt{\sigma_m\Upsilon^m_t}\bar{D}_i\},$$
$$\tilde{E}^T_{\Omega^a_{uk}\Lambda^c_{uk}\Upsilon^m_k} = \left[\bar{E}^T_{\Omega^a_{uk}\Lambda^c_{uk}\Upsilon^m_k}\ \bar{E}^T_{\Omega^a_{uk}\Lambda^c_{uk}\Upsilon^m_k}\ \bar{E}^T_{\Omega^a_{uk}\Lambda^c_{uk}\Upsilon^m_k}\right],$$
$$\bar{E}^T_{\Omega^a_{uk}\Lambda^c_{uk}\Upsilon^m_k} = [\sqrt{\sigma_m\Upsilon^m_1}\hat{E}^T \cdots \sqrt{\sigma_m\Upsilon^m_t}\hat{E}^T],$$
$$\Psi_{\Omega^a_{u\ell}\Lambda^c_{u\ell}\Upsilon^m_{u\ell}} = diag\left\{\tilde{\Psi}_{\Omega^a_{u\ell}\Lambda^c_{u\ell}\Upsilon^m_{u\ell}}\ \tilde{\Psi}_{\Omega^a_{u\ell}\Lambda^c_{u\ell}\Upsilon^m_{u\ell}}\ \tilde{\Psi}_{\Omega^a_{u\ell}\Lambda^c_{u\ell}\Upsilon^m_{u\ell}}\right\},$$
$$\tilde{\Psi}_{\Omega^a_{uk}\Lambda^c_{uk}\Upsilon^m_{uk}} = diag\{-S_{bdn} \cdots - S_{bdn}\},$$
$$X^T_{\Omega^a_{uk}\Lambda^c_{uk}\Upsilon^m_{uk}} = \left[\check{X}^T_{1\Omega^a_{uk}\Lambda^c_{uk}\Upsilon^m_{uk}}\ \check{X}^T_{2\Omega^a_{uk}\Lambda^c_{uk}\Upsilon^m_{uk}}\ \check{X}^T_{3\Omega^a_{uk}\Lambda^c_{uk}\Upsilon^m_{uk}}\right],$$
$$\check{X}^T_{i\Omega^a_{uk}\Lambda^c_{uk}\Upsilon^m_{uk}} = [\tilde{\eta}^T_i \cdots \tilde{\eta}^T_i],$$
$$\tilde{D}_{\Omega^a_{u\ell}\Lambda^c_{u\ell}\Upsilon^m_{uk}} = diag\left\{\tilde{D}_{1\Omega^a_{uk}\Lambda^c_{uk}\Upsilon^m_{uk}}\ \tilde{D}_{2\Omega^a_{uk}\Lambda^c_{uk}\Upsilon^m_{uk}}\ \tilde{D}_{3\Omega^a_{uk}\Lambda^c_{uk}\Upsilon^m_{uk}}\right\},$$
$$\tilde{D}_{i\Omega^a_{uk}\Lambda^c_{uk}\Upsilon^m_{uk}} = diag\{\bar{D}_i \cdots \bar{D}_i\},\ (i = 1, 2, 3),$$
$$\tilde{E}^T_{\Omega^a_{uk}\Lambda^c_{uk}\Upsilon^m_{uk}} = \left[\bar{E}^T_{\Omega^a_{uk}\Lambda^c_{uk}\Upsilon^m_{uk}}\ \bar{E}^T_{\Omega^a_{uk}\Lambda^c_{uk}\Upsilon^m_{uk}}\ \bar{E}^T_{\Omega^a_{uk}\Lambda^c_{uk}\Upsilon^m_{uk}}\right],$$
$$\bar{E}^T_{\Omega^a_{uk}\Lambda^c_{uk}\Upsilon^m_{uk}} = [\hat{E}^T \cdots \hat{E}^T],$$

B. DEFINITION OF PARAMETERS IN (41)

$$\tilde{\Xi}_0 = \begin{bmatrix} \Xi_{11} & * & * & * \\ \Xi_{210} & \Xi_{22} & * & * \\ \Xi_{310} & 0 & \Xi_{33} & * \\ \Xi_{410} & 0 & 0 & \Xi_{44} \end{bmatrix},$$
$$\Xi_{210} = \phi_M X_0,\ \Xi_{310} = \varphi_M X_0,\ \Xi_{410} = \psi_M X_0,$$
$$X_0 = \begin{bmatrix} (\tilde{A}_0 - I) & \bar{\alpha}I_1L\tilde{C} & \tilde{B}_0KI_2 & \bar{\beta}\hat{B}_0KI_3 & 0\,0\,0 \\ 0 & \alpha_1I_1L\tilde{C} & 0 & 0 & 0\,0\,0 \\ 0 & 0 & 0 & \beta_1\hat{B}_0KI_3 & 0\,0\,0 \end{bmatrix},$$
$$X^T_{\Omega^a_k\Lambda^c_k\Upsilon^m_k} = \left[\check{X}^T_{1\Omega^a_k\Lambda^c_k\Upsilon^m_k}\ \check{X}^T_{2\Omega^a_k\Lambda^c_k\Upsilon^m_k}\ \check{X}^T_{3\Omega^a_k\Lambda^c_k\Upsilon^m_k}\right],$$
$$\check{X}^T_{i\Omega^a_k\Lambda^c_k\Upsilon^m_k} = [\sqrt{\mu_a\Omega^a_1\nu_c\Lambda^c_1\sigma_m\Upsilon^m_1}\tilde{\eta}^T_i \cdots \sqrt{\mu_a\Omega^a_p\nu_c\Lambda^c_r\sigma_m\Upsilon^m_t}\tilde{\eta}^T_i],$$
$$\tilde{\eta}_1 = \left[\eta_{10}\ 0\ 0\ 0\right],\quad \tilde{\eta}_2 = \left[\eta_{20}\ 0\ 0\ 0\right],$$
$$\tilde{\eta}_3 = \left[\eta_{30}\ 0\ 0\ 0\right],$$
$$\eta_{10} = \left[\tilde{A}_0\ \bar{\alpha}I_1L\tilde{C}\ \tilde{B}_0\ KI_2\ \bar{\beta}\hat{B}_0\ KI_3\ 0\ 0\ 0\right],$$
$$\eta_{20} = \left[0\ \alpha_1I_1L\tilde{C}\ 0\ 0\ 0\ 0\ 0\right],$$
$$\eta_{30} = \left[0\ 0\ 0\ \beta_1\hat{B}_0\ KI_3\ 0\ 0\ 0\right].$$
$$D_{\Omega^a_k\Lambda^c_k\Upsilon^m_k} = \begin{bmatrix} \tilde{D} & 0 \\ 0 & \tilde{D}_{\Omega^a_k\Lambda^c_k\Upsilon^m_k} \end{bmatrix},$$
$$\tilde{D} = diag\left\{0, \phi_M\mu\nu\sigma\hat{D}, \varphi_M\mu\nu\sigma\hat{D}, \psi_M\mu\nu\sigma\hat{D}\right\},$$
$$\hat{D} = \begin{bmatrix} \tilde{D}_1 & \tilde{D}_2 & \bar{\beta}\tilde{D}_3 \\ 0 & 0 & 0 \\ 0 & 0 & \beta_1\tilde{D}_3 \end{bmatrix},$$
$$\tilde{D}_{\Omega^a_k\Lambda^c_k\Upsilon^m_k} = diag\left\{\tilde{D}_{1\Omega^a_k\Lambda^c_k\Upsilon^m_k}\ \tilde{D}_{2\Omega^a_k\Lambda^c_k\Upsilon^m_k}\ \tilde{D}_{3\Omega^a_k\Lambda^c_k\Upsilon^m_k}\right\},$$
$$\tilde{D}_{i\Omega^a_k\Lambda^c_k\Upsilon^m_k} = diag\{\sqrt{\mu_a\Omega^a_1\nu_c\Lambda^c_1\sigma_m\Upsilon^m_1}\bar{D}_i \cdots \sqrt{\mu_a\Omega^a_p\nu_c\Lambda^c_r\sigma_m\Upsilon^m_t}\bar{D}_i\},\ (i = 1, 2, 3),$$
$$E_{\Omega^a_k\Lambda^c_k\Upsilon^m_k} = \begin{bmatrix} \tilde{E} & 0 \\ \tilde{E}_{\Omega^a_k\Lambda^c_k\Upsilon^m_k} & 0 \end{bmatrix},\quad \tilde{E}^T = \left[0\ \hat{E}^T\ \hat{E}^T\ \hat{E}^T\right],$$
$$\hat{E} = \left[\bar{E}\ 0\ 0\ 0\right],$$
$$\bar{E} = \begin{bmatrix} \tilde{E}_1 & 0 & 0 & 0 & 0\,0\,0 \\ 0 & 0 & \tilde{E}_2KI_2 & 0 & 0\,0\,0 \\ 0 & 0 & 0 & \tilde{E}_3KI_3 & 0\,0\,0 \end{bmatrix},$$
$$\tilde{E}^T_{\Omega^a_k\Lambda^c_k\Upsilon^m_k} = \left[\bar{E}^T_{\Omega^a_k\Lambda^c_k\Upsilon^m_k}\ \bar{E}^T_{\Omega^a_k\Lambda^c_k\Upsilon^m_k}\ \bar{E}^T_{\Omega^a_k\Lambda^c_k\Upsilon^m_k}\right],$$
$$\bar{E}^T_{\Omega^a_k\Lambda^c_k\Upsilon^m_k} = \left[\sqrt{\mu_a\Omega^a_1\nu_c\Lambda^c_1\sigma_m\Upsilon^m_1}\hat{E}^T \cdots \sqrt{\mu_a\Omega^a_p\nu_c\Lambda^c_r\sigma_m\Upsilon^m_t}\hat{E}^T\right],$$
$$F = \begin{bmatrix} \hat{F} & 0 \\ 0 & F_{\Omega^a_k\Lambda^c_k\Upsilon^m_k} \end{bmatrix},\quad \hat{F} = diag\left\{0, \tilde{F}, \tilde{F}, \tilde{F}\right\},$$
$$F_{\Omega^a_k\Lambda^c_k\Upsilon^m_k} = diag\left\{\tilde{F} \cdots \tilde{F}\right\},\quad \tilde{F} = diag\left\{\tilde{F}_1\ \tilde{F}_2\ \tilde{F}_3\right\},$$

REFERENCES

[1] R. A. Gupta and M.-Y. Chow, "Networked control system: Overview and research trends," *IEEE Trans. Ind. Electron.*, vol. 57, no. 7, pp. 2527–2535, Jul. 2010.

[2] Y. Xia, "From networked control systems to cloud control systems," in *Proc. 31st Chin. Control Conf.*, Jul. 2012, pp. 5878–5883.

[3] Y. Zhan, Y. Xia, and A. V. Vasilakos, "Future directions of networked control systems: A combination of cloud control and fog control approach," *Comput. Netw.*, vol. 161, pp. 235–248, Oct. 2019.

[4] Q. Zhang, L. Cheng, and R. Boutaba, "Cloud computing: State-of-the-art and research challenges," *J. Internet Services Appl.*, vol. 1, no. 1, pp. 7–18, May 2010.

[5] M. A. Vouk, "Cloud computing–issues, research and implementations," *J. Comput. Inf. Technol.*, vol. 16, no. 4, pp. 235–246, 2008.

[6] S. S. Manvi and G. Krishna Shyam, "Resource management for infrastructure as a service (IaaS) in cloud computing: A survey," *J. Netw. Comput. Appl.*, vol. 41, pp. 424–440, May 2014.

[7] M. Cusumano, "Cloud computing and SaaS as new computing platforms," *Commun. ACM*, vol. 53, no. 4, pp. 27–29, Apr. 2010.

[8] B. Hayes, "Cloud computing," *Commun. ACM*, vol. 51, no. 7, pp. 9–11, Jul. 2008.

[9] M. S. Mahmoud and Y. Xia, "The interaction between control and computing theories: New approaches," *Int. J. Autom. Comput.*, vol. 14, no. 3, pp. 254–274, Apr. 2017.

[10] Y. Xia, "Cloud control systems and their challenges," *Acta Autom. Sinica*, vol. 42, no. 1, pp. 1–12, 2016.

[11] O. Givehchi, J. Imtiaz, H. Trsek, and J. Jasperneite, "Control-as-a-service from the cloud: A case study for using virtualized PLCs," in *Proc. 10th IEEE Workshop Factory Commun. Syst. (WFCS)*, May 2014, pp. 1–4.

[12] H. Esen, M. Adachi, D. Bernardini, A. Bemporad, D. Rost, and J. Knodel, "Control as a service (CaaS): Cloud-based software architecture for automotive control applications," in *Proc. 2nd Int. Workshop Swarm at Edge Cloud*, Apr. 2015, pp. 13–18.

[13] S. Mubeen, P. Nikolaidis, A. Didic, H. Pei-Breivold, K. Sandstrom, and M. Behnam, "Delay mitigation in offloaded cloud controllers in industrial IoT," *IEEE Access*, vol. 5, pp. 4418–4430, 2017.

[14] T. Hegazy and M. Hefeeda, "Industrial automation as a cloud service," *IEEE Trans. Parallel Distrib. Syst.*, vol. 26, no. 10, pp. 2750–2763, Oct. 2015.

[15] A. Tchernykh, U. Schwiegelsohn, V. Alexandrov, and E.-G. Talbi, "Towards understanding uncertainty in cloud computing resource provisioning," *Procedia Comput. Sci.*, vol. 51, pp. 1772–1781, Jan. 2015.

[16] P. Saikrishna and R. Pasumarthy, "Multi-objective switching controller for cloud computing systems," *Control Eng. Pract.*, vol. 57, pp. 72–83, Dec. 2016.

[17] Y. Xia, "Cloud control systems," *IEEE/CAA J. Automatica Sinica*, vol. 2, no. 2, pp. 134–142, Apr. 2015.

[18] Y. Xia, Y. Qin, D.-H. Zhai, and S. Chai, "Further results on cloud control systems," *Sci. China Inf. Sci.*, vol. 59, no. 7, Jul. 2016, Art. no. 073201.
[19] M. S. Mahmoud, "Architecture for cloud-based industrial automation," in *Proc. 3rd Int. Congr. Inf. Commun. Technol.* Cham, Switzerland: Springer, 2019, pp. 51–62.
[20] M. S. Mahmoud, "Cloud-based control systems: Basics and beyond," *J. Phys., Conf. Ser.*, vol. 1334, Oct. 2019, Art. no. 012006.
[21] Y. Ali, Y. Xia, L. Ma, and A. Hammad, "Secure design for cloud control system against distributed denial of service attack," *Control Theory Technol.*, vol. 16, no. 1, pp. 14–24, Feb. 2018.
[22] H. Yuan, Y. Xia, M. Lin, H. Yang, and R. Gao, "Dynamic pricing-based resilient strategy design for cloud control system under jamming attack," *IEEE Trans. Syst., Man, Cybern. Syst.*, vol. 50, no. 1, pp. 111–122, Jan. 2020.
[23] H. Yuan, Y. Xia, J. Zhang, H. Yang, and M. S. Mahmoud, "Stackelberg-game-based defense analysis against advanced persistent threats on cloud control system," *IEEE Trans. Ind. Informat.*, vol. 16, no. 3, pp. 1571–1580, Mar. 2020.
[24] H. Tan, Z. Huang, and M. Wu, "An interactive real-time SCADA platform with customizable virtual instruments for cloud control systems," *J. Dyn. Syst., Meas., Control*, vol. 141, no. 4, Apr. 2019, Art. no. 044501.
[25] C.-L. Wang, Y.-G. Tao, P. Yang, Z.-J. Liu, and Y. Zhou, "Parallel task assignment optimization algorithm and parallel control for cloud control systems," *Acta Autom. Sinica*, vol. 43, no. 11, pp. 1973–1983, 2017.
[26] J. Schlechtendahl, F. Kretschmer, Z. Sang, A. Lechler, and X. Xu, "Extended study of network capability for cloud based control systems," *Robot. Comput.-Integr. Manuf.*, vol. 43, pp. 89–95, Feb. 2017.
[27] H. Wu, L. Lou, C.-C. Chen, S. Hirche, and K. Kuhnlenz, "Cloud-based networked visual servo control," *IEEE Trans. Ind. Electron.*, vol. 60, no. 2, pp. 554–566, Feb. 2013.
[28] Q. Ding and S. Cao, "RECT: A cloud-based learning tool for graduate software engineering practice courses with remote tutor support," *IEEE Access*, vol. 5, pp. 2262–2271, 2017.
[29] L. Xu, D. Huang, and W.-T. Tsai, "Cloud-based virtual laboratory for network security education," *IEEE Trans. Educ.*, vol. 57, no. 3, pp. 145–150, Aug. 2014.
[30] M. Shengdong, X. Zhengxian, and T. Yixiang, "Intelligent traffic control system based on cloud computing and big data mining," *IEEE Trans. Ind. Informat.*, vol. 15, no. 12, pp. 6583–6592, Dec. 2019.
[31] Y.-Q. Xia, C. Yan, X.-J. Wang, and X. Song, "Intelligent transportation cyber-physical cloud control systems," *Acta Autom. Sinica*, vol. 45, no. 1, pp. 132–142, 2019.
[32] G. Hu, W. Tay, and Y. Wen, "Cloud robotics: Architecture, challenges and applications," *IEEE Netw.*, vol. 26, no. 3, pp. 21–28, May 2012.
[33] C. Okwudire, S. Huggi, S. Supe, C. Huang, and B. Zeng, "Low-level control of 3D printers from the cloud: A step toward 3D printer control as a service," *Inventions*, vol. 3, no. 3, p. 56, Aug. 2018.
[34] S. Guan and S. Niu, "Stability-based controller with uncertain parameters for cloud control system," in *Proc. Chin. Control Decis. Conf. (CCDC)*, Aug. 2020, pp. 3842–3846.
[35] W. He, T. Wang, X. He, L.-J. Yang, and O. Kaynak, "Dynamical modeling and boundary vibration control of a rigid-flexible wing system," *IEEE/ASME Trans. Mechatronics*, vol. 25, no. 6, pp. 2711–2721, Dec. 2020.
[36] L. Liu, Y.-J. Liu, A. Chen, S. Tong, and C. L. P. Chen, "Integral barrier Lyapunov function-based adaptive control for switched nonlinear systems," *Sci. China Inf. Sci.*, vol. 63, no. 3, pp. 1–14, Mar. 2020.
[37] L. Liu, Y.-J. Liu, D. Li, S. Tong, and Z. Wang, "Barrier Lyapunov function-based adaptive fuzzy FTC for switched systems and its applications to resistance–inductance–capacitance circuit system," *IEEE Trans. Cybern.*, vol. 50, no. 8, pp. 3491–3502, Aug. 2020.
[38] L. Ma, Y. Xia, Y. Ali, and Y. Zhan, "Engineering problems in initial phase of cloud control system," in *Proc. 36th Chin. Control Conf. (CCC)*, Jul. 2017, pp. 7892–7896.
[39] N. Popović and M. Naumović, "Networked and cloud control systems–modern challenges in control engineering," *IJEEC-Int. J. Electr. Eng. Comput.*, vol. 2, no. 2, pp. 91–100, Mar. 2019.
[40] A. Selivanov and E. Fridman, "Observer-based input-to-state stabilization of networked control systems with large uncertain delays," *Automatica*, vol. 74, pp. 63–70, Dec. 2016.
[41] H. Zhang, Y. Shi, J. Wang, and H. Chen, "A new delay-compensation scheme for networked control systems in controller area networks," *IEEE Trans. Ind. Electron.*, vol. 65, no. 9, pp. 7239–7247, Sep. 2018.
[42] X. Ge, F. Yang, and Q.-L. Han, "Distributed networked control systems: A brief overview," *Inf. Sci.*, vol. 380, pp. 117–131, Feb. 2017.
[43] Y. Wang, P. He, H. Li, X. Sun, H. Mi, W. Wei, X. Xiong, and Y. Li, "H_∞ control of networked control system with data packet dropout via observer-based controller," *IEEE Access*, vol. 8, pp. 58300–58309, 2020.
[44] Y. Wang, P. He, H. Li, X. Sun, W. Wei, Z. Wei, and Y. Li, "Stabilization for networked control system with time-delay and packet loss in both S-C side and C–A side," *IEEE Access*, vol. 8, pp. 2513–2523, 2020.
[45] R. Yang, G.-P. Liu, P. Shi, C. Thomas, and M. V. Basin, "Predictive output feedback control for networked control systems," *IEEE Trans. Ind. Electron.*, vol. 61, no. 1, pp. 512–520, Jan. 2014.
[46] M. B. G. Cloosterman, N. van de Wouw, W. P. M. H. Heemels, and H. Nijmeijer, "Stability of networked control systems with uncertain time-varying delays," *IEEE Trans. Autom. Control*, vol. 54, no. 7, pp. 1575–1580, Jul. 2009.
[47] A. Farnam and R. Mahboobi Esfanjani, "Improved stabilization method for networked control systems with variable transmission delays and packet dropout," *ISA Trans.*, vol. 53, no. 6, pp. 1746–1753, Nov. 2014.
[48] A. Tchernykh, U. Schwiegelsohn, E.-G. Talbi, and M. Babenko, "Towards understanding uncertainty in cloud computing with risks of confidentiality, integrity, and availability," *J. Comput. Sci.*, vol. 36, Sep. 2019, Art. no. 100581.
[49] G.-P. Liu, "Predictive control of networked multiagent systems via cloud computing," *IEEE Trans. Cybern.*, vol. 47, no. 8, pp. 1852–1859, Aug. 2017.
[50] S. Singh, Y.-S. Jeong, and J. H. Park, "A survey on cloud computing security: Issues, threats, and solutions," *J. Netw. Comput. Appl.*, vol. 75, pp. 200–222, Nov. 2016.
[51] W.-J. Mao and J. Chu, "Quadratic stability and stabilization of dynamic interval systems," *IEEE Trans. Autom. Control*, vol. 48, no. 6, pp. 1007–1012, Jun. 2003.
[52] Y. Shi and B. Yu, "Output feedback stabilization of networked control systems with random delays modeled by Markov chains," *IEEE Trans. Autom. Control*, vol. 54, no. 7, pp. 1668–1674, Jul. 2009.
[53] X. Jiang, Q.-L. Han, and X. Yu, "Stability criteria for linear discrete-time systems with interval-like time-varying delay," in *Proc. Amer. Control Conf.*, Jun. 2005, pp. 2817–2822.
[54] Z. Wang, F. Yang, D. W. C. Ho, and X. Liu, "Robust H_∞ control for networked systems with random packet losses," *IEEE Trans. Syst., Man, Cybern. B, Cybern.*, vol. 37, no. 4, pp. 916–924, Aug. 2007.
[55] A.-W.-A. Saif, "New results on the observer-based H_∞ control for uncertain nonlinear networked control systems with random packet losses," *IEEE Access*, vol. 7, pp. 26179–26191, 2019.
[56] S. Guan and X. Dong, "An architecture of cloud control system and its application in greenhouse environment," in *Proc. Chin. Control Conf. (CCC)*, Jul. 2019, pp. 2829–2834.

SHOUPING GUAN received the B.S. and M.S. degrees in automatic control from the Harbin Shipbuilding Engineering Institute, Harbin, China, in 1989 and 1992, respectively, and the Ph.D. degree in control engineering from Northeastern University, Shenyang, China, in 1995.

He is currently a Professor with the College of Information Science and Engineering, Northeastern University. His research interests include intelligent control, precision measurement and control, modeling, and optimization of industrial process.

SENLIN NIU received the B.S. degree in automation from Yanshan University, Qinhuangdao, China, in 2018. He is currently pursuing the master's degree in control theory and control engineering with Northeastern University, Shenyang, China.

His research interests include modeling, optimization, and control of complex industrial processes.